

From: "Davis, James T." <JTDAVIS@southernco.com>
To: "Christian Araguas" <CJA2@nrc.gov>
Date: 4/16/2007 6:08:12 PM
Subject: RAI Letter #6 Geology Response 2 of 3

<<AR-07-0801_2 of 3.pdf>>

Jim Davis
Southern Nuclear
ESP Project Engineer
205.992.7692 Office
205.253.1248 Cell
205.992.5296 Fax
Mailing Address
Post Office Box 1295, BIN B056
Birmingham, AL 35201
Street Address
Building 40
Inverness Center Parkway
Birmingham, AL 35242

Hearing Identifier: Vogtle_Public
Email Number: 354

Mail Envelope Properties (463F419B.HQGWDO01.TWGWPO04.200.2000016.1.B01CC.1)

Subject: RAI Letter #6 Geology Response 2 of 3
Creation Date: 4/16/2007 6:08:12 PM
From: "Davis, James T." <JTDAVIS@southernco.com>

Created By: JTDAVIS@southernco.com

Recipients
"Christian Araguas" <CJA2@nrc.gov>

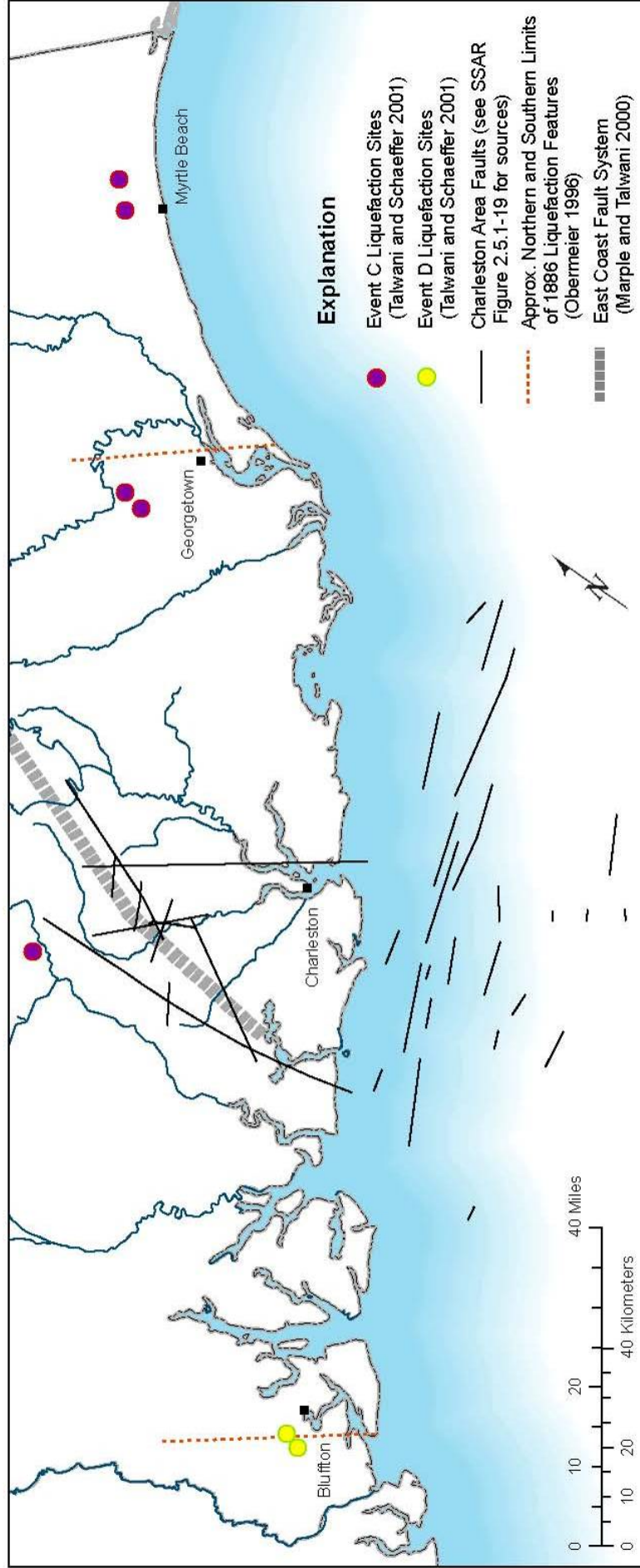
Post Office
TWGWPO04.HQGWDO01

Route
nrc.gov

Files	Size	Date & Time
MESSAGE	296	4/16/2007 6:08:12 PM
AR-07-0801_2 of 3.pdf	3783223	5/7/2007 3:11:23 PM
Mime.822	5298183	5/7/2007 3:11:23 PM

Options
Priority: Standard
Reply Requested: No
Return Notification: None
None

Concealed Subject: No
Security: Standard



RAI Figure 2.5.2-11, Liquefaction Sites for Events C, C, and D

2.5.2-12 SSAR Section 2.5.2.2.2.4.3 describes the calculation of two average recurrence intervals covering two different time intervals, which are used as two recurrence branches on the logic tree. Please justify in greater detail your rationale for the weighting of the two recurrence branches on the logic tree.

In addition, please justify your use of these two scenarios rather than another case study (for example, ten large-magnitude earthquakes occurring at approximately regular intervals during the past 5,000 years), including its impact on the hazard calculation you could have considered.

Response:

The calculation of average recurrence intervals for Charleston seismic source M_{\max} earthquakes performed for the VEGP ESP application is based largely on paleoliquefaction data compiled by Talwani and Schaeffer (2001). Using these data, two average recurrence intervals covering two different time intervals were calculated. The first recurrence interval is based on the most-recent ~2,000-yr record of paleoliquefaction events and is given a 0.80 weight in the logic tree. The second recurrence interval is based on the entire ~5,000-yr record of paleoliquefaction events and is given a 0.20 weight in the logic tree. The entire ~5,000-yr record and the ~2,000-yr subset were used to calculate separate recurrence intervals in order to capture varying degrees of confidence expressed by experts regarding the relative completeness of different portions of the geologic record.

The relative weighting of these two branches of the logic tree is based on a SSHAC level 2 assessment of completeness of the geologic record of paleoliquefaction events over these two time intervals. Earthquakes in the paleoliquefaction record do not occur at regular intervals, and this may be the result of “temporal clustering of seismicity, fluctuation of water levels, or their evidence having been obliterated” (Talwani and Schaeffer 2001; p. 6640). Talwani and Schaeffer (2001) consider the paleoliquefaction record to be complete for the past 2,000 yrs. Moreover, Prof. Pradeep Talwani (University of South Carolina, pers. comm. 9/8/05) and Dr. Steve Obermeier (U.S. Geological Survey [retired], pers. comm. 9/2/05) consider the 2,000-yr record to represent a complete portion of the paleoseismic record. For these reasons, the average recurrence interval calculated for the most-recent ~2,000 yr portion of the paleoseismologic record is given a relatively high weight of 0.80.

The degree of completeness for the entire ~5,000-yr record of paleoliquefaction events is uncertain. It is possible that all paleoliquefaction events in this time period have been preserved and recognized in the geologic record. Alternatively, it is possible that events are missing from the ~5,000-yr record. Average M_{\max} recurrence interval calculated from the entire ~5,000-yr record is greater (i.e., larger average inter-event time) than that calculated for the ~2,000-yr record. The decision to give less weight (0.20) to this recurrence estimate is therefore conservative.

We also considered other scenarios from which to calculate earthquake recurrence, but ultimately decided not to incorporate those that included non-conservative assumptions. For example, Talwani and Schaeffer (2001) include a scenario in which their events C and D are moderate-magnitude, local earthquakes. These moderate-magnitude earthquakes would be eliminated from the record of large (M_{\max}) earthquakes, thereby increasing the calculated recurrence interval. This and other permutations of the paleoliquefaction record (and resulting recurrence intervals) could be included, but, if based on non-conservative assumptions, would increase the recurrence interval and lower the hazard without sufficient justification.

The given example of “ten large-magnitude earthquakes occurring at approximately regular intervals during the past 5,000 years” was not included in the model because: (1) it is permissible only if events are assumed to be missing from the geologic record, and (2) the resulting recurrence interval would be very similar to the branch of the logic tree using the ~2,000-yr paleoliquefaction record.

2.5.2-13 SSAR Section 2.5.2.4.4 states that "the new interpretation of the Charleston source indicates that a source of the large earthquakes in the Charleston area exists with weight 1.0..." Although the UCSS update of the Charleston source zone covers a fairly large area, the weighting and source geometries give the largest hazard only inside Zone A (either 0.9 (A, B, B') or 1.0 (A, B, B', C)), which is a relatively small zone. In view of this result, provide justification for the UCSS source geometries and weighting scheme and define what is meant by the "Charleston area".

Response:

As part of the VEGP ESP application, a SSHAC level 2 committee characterized source parameters of the Charleston seismic source. This committee assessed that the preponderance of evidence strongly supports the conclusion that the seismic source for the 1886 and prehistoric Charleston earthquakes is stationary in space. In other words, the source area that produces 1886 Charleston-type large-magnitude earthquakes is likely relatively restricted in area.

The updated Charleston seismic source model includes four potential geometries (A, B, B', and C) to represent the source area for the Charleston seismic source zone. The greatest weight is given to a localized zone (Geometry A) that completely incorporates the 1886 earthquake Modified Mercalli Intensity (MMI) X isoseismal (Bollinger 1977), the majority of identified Charleston meizoseismal-area tectonic features and inferred fault intersections, and the majority of reported 1886 liquefaction features. Outlying liquefaction features are excluded because liquefaction occurs as a result of strong ground shaking that may extend well beyond the areal extent of the tectonic source. Data describing the size and spatial distribution of paleoliquefaction features suggest prehistoric earthquakes (Events A, B, C', E, and F') were of similar magnitude and location to the 1886 Charleston earthquake, which produced liquefaction at significant distances northeast and southwest from the meizoseismal area. Lower weights are given for source geometries that envelop specific postulated tectonic features (i.e., Geometry C for the southern segment of the East Coast fault system), or for broader areal distributions that also envelop the localized zone to allow for greater uncertainty in the location and lateral extent of a fault that may have produced the 1886 Charleston earthquake.

The term “Charleston area” as used in the third sentence of the first paragraph of Section 2.5.2.4.4 is vague and the following wording is proposed for the next revision of the ESP application:

The new interpretation of the Charleston source (see Section 2.5.2.2.2) indicates that a unique source of large earthquakes exists with weight 1.0 and that large magnitude events occur with a rate of occurrence unrelated to the rate of smaller magnitudes.

The next revision to the ESP application will address as appropriate the information provided in this response.

2.5.2-14 SSAR Section 2.5.2.2.2.4.1 states that the width of Geometry B is 80 km (50 miles). However, SSAR Figure 2.5.2-9 shows the width of Geometry B to be approximately 100 km (62 miles). Please provide the actual dimensions of Geometry B used for the UCSS.

Response:

The reviewer is correct. The width of UCSS geometry B is 100 km as pointed out by the reviewer, not 80 km as stated in Section 2.5.2.2.2.4.1. This is a typographical error that will be corrected in the next revision of the ESP application.

2.5.2-15 As stated in SSAR Section 2.5.2.2.2.4.1, the offshore Helena Banks fault zone was detected by multiple seismic reflection profiles. Please explain why the two seismic events (mb 3.5 and 4.4) in 2002, which occurred in the vicinity of the Helena Bank fault system, cannot be positively correlated with the fault zone, and did not demonstrate recent activity for the fault zone. Could the seismicity symbolize the reactivation of the Helena Bank fault zone?

Response:

In 2002, two earthquakes (m_b 3.5 and 4.4) occurred off the coast of South Carolina in the vicinity of the Helena Banks fault zone in an area previously devoid of seismicity. Whereas we cannot entirely rule out the possibility that the Helena Banks fault zone produced these two earthquakes, neither can we positively correlate these two earthquakes with the Helena Banks fault for the following three reasons:

1. Large uncertainty in the location of these events. Small offshore earthquakes like those in question are typically difficult to locate accurately given the asymmetric distribution of recording stations relative to the hypocenters (the instrumentation is confined to land). Positional uncertainties for earthquakes in the updated EPRI catalog are not stated, but it is likely that the horizontal uncertainties for the two 2002 offshore South Carolina earthquakes are on the order of a few miles. For this reason it is not possible to attribute these small earthquakes to any fault or faults within the Helena Banks fault zone.
2. Events do not define a swarm or lineament of seismicity that can be used to define orientation and/or geometry of any causative fault. The two 2002 earthquakes occurred in approximately the same location, therefore making it difficult to deduce an orientation for the causative fault (if, in fact, the two earthquakes were produced by the same feature).
3. Lack of focal mechanisms. Focal mechanisms, when available, can be used to help define fault orientation and sense-of-slip on the causative fault. Focal mechanisms for the events in question, however, are not available.

The lack of detailed information on these two 2002 offshore earthquakes (poor location, no focal mechanisms) and the lack of additional seismic activity in this offshore area, make it difficult to assign the Helena Banks fault zone as the causative fault. It is possible that the two 2002 earthquakes indicate reactivation of the Helena Banks fault zone, but the fact that these events cannot be positively correlated to the fault suggests otherwise. There are numerous faults in the central and eastern United States located close to a few or more poorly located, small earthquakes, but this simple and very limited spatial association has not typically led researchers to positively correlate them to specific faults and classify these faults as reactivated seismogenic structures.

2.5.2-16 SSAR Section 2.5.2.2.2.5 discusses the Eastern Tennessee Seismic Zone (ETSZ). Please provide, electronically, the geographic coordinates defining the geometry of the Eastern Tennessee Seismic Zone (ETSZ) seismic source zones and associated seismicity parameters (including Mmax magnitude distributions) for each EPRI-SOG EST.

Response:

None of the EPRI-SOG teams specifically defined a zone identified as “Eastern Tennessee Seismic Zone.” Each EPRI-SOG team did define one or more zones that encompass seismicity in eastern Tennessee and, in most cases, surrounding regions. These zones were as follows:

<u>Team</u>	<u>Zone number</u>	<u>Zone name</u>
Bechtel:	24	Bristol trends
	25	NY-AL lineament
	25A	NY-AL lineament (alternative)
Dames & Moore	04	Appalachian fold belt
	4A	Kinds in Appalachian fold belt
Law Engineering	17	Eastern basement
Rondout	13	So. NY-AL lineament
	25	So. Appalachians
	27	TN-VA border
Weston Geophysical	24	NY-AL Clingman
Woodward-Clyde	31	Blue Ridge comb.
	31A	Blue Ridge comb. (alternative)

The geometries for these 12 sources are included in an electronic file in Enclosure 2 to this letter labeled “252-16_geom.txt”. Also, the maximum magnitude distributions for these sources are included in an electronic file in Enclosure 2 to this letter labeled “252-16_mmax.xls.” We understand from a telephone conference call conducted with the NRC on March 9, 2007, that associated seismicity parameters will not be required because they are specified by degree cell within each source, and this information would be voluminous.

2.5.2-17 SSAR Section 2.5.2.2.2.5 discusses the Eastern Tennessee Seismic Zone (ETSZ). Please justify in greater detail your rationale for not updating the ETSZ as characterized by the EPRI ESTs. In addition, please discuss how the Mmax magnitude distributions developed by each EST compare with more recent Mmax estimates by the USGS hazard model (Frankel et al. 2002) and Bollinger (1992).

SSAR Section 2.5.2.2.2.5 states that the ETSZ does not contribute significantly to the hazard at the VEGP site. Please explain whether and how this would change if the EST’s source zones representing the ETSZ were assigned a single Mmax of Mw 7.5. Alternatively, explain why you believe an Mmax value of Mw 7.5 with a weight of 0.5 or higher is not warranted for the ETSZ.

Response:

The reasons for not revising the EPRI ETSZ source characterizations for the Vogtle ESP are summarized as follows:

- (1) The majority of seismicity that defines the ETSZ is beyond the 200-mi site region. The Clingman and Ocoee geophysical lineaments that define the southeastern boundary of the Ocoee block and the bulk of ETSZ seismicity lie about 170 mi and 195 mi, respectively, northwest of the VEGP site. The USGS representation of the ETSZ (Frankel et al. 1996, 2002) lies about 200 mi northwest of the VEGP site.
- (2) The revision of the Charleston seismic source recurrence from a few thousand years in the EPRI SOG model to several hundred years (based on paleoliquefaction evidence) has increased the relative contribution of the Charleston source to the VEGP site. The increase in hazard contribution from the Charleston source serves to decrease the relative contribution of more distant sources such as the ETSZ.
- (3) The largest recorded earthquake within the ETSZ is about “magnitude 4.6” (Chapman et al. 2002). The recent Fort Payne, AL earthquake of April 29, 2003 that occurred near the southwestern limit of ETSZ seismicity was also a magnitude 4.6. Unlike other zones of significant seismicity in the CEUS, there is no historic or prehistoric evidence for large magnitude events occurring in the eastern Tennessee area. Seismic sources that model earthquake activity in Charleston and New Madrid have been assigned large M_{\max} values both by EPRI ESTs and more recent PSHA studies, because of the occurrence of large historical earthquakes. In addition, these areas also exhibit abundant evidence for prehistoric, large magnitude earthquakes in the form of paleoliquefaction features. Evidence documenting large earthquakes in the geologic record has yet to be found in the eastern Tennessee area. While the lack of evidence for past large events in ETSZ does not preclude large events from occurring in the future, this fact should influence the weighting of the M_{\max} distribution. It is therefore logical that the M_{\max} distribution for the ETSZ should have lower weights assigned to the largest magnitudes, in contrast to the Charleston and New Madrid sources, where there is a high confidence that those sources are capable of producing large events since they have occurred in the past.
- (4) The EPRI SOG maximum magnitude distributions for the ETSZ span the range of more recent assessments.

More recent estimates of maximum magnitudes for the ETSZ include Bollinger (1992) and the USGS source models for the national hazard maps (Frankel et al. 2002). In developing a source model for the Savannah River Site (SRS), Bollinger (1992) used three methods to estimate maximum magnitude by (1) determining the 1,000-year earthquake, (2) adding 1.0 magnitude increment to the maximum historical event, and (3) using fault zone area. The average of these three estimates for the ETSZ is reported by Bollinger as m_b 6.45, which converts to M 6.3 using the average of three relations tabulated in the response to RAI 2.5.2-5. The fault zone dimensions included in this average were restricted to causative faults assumed to be oriented north-south and east-west within the ETSZ, parallel to measured focal mechanism nodal planes. In addition, Bollinger (1992) assumed a low probability that the dimensions of seismogenic structures within the zone may extend along the entire 300-km-long northeast trending axis of the zone, and therefore, the ETSZ could be capable of producing a New Madrid size earthquake. He defined a second ETSZ source zone of the same dimensions as the primary source and assigned an M_{\max} of m_b 7.35 (M 7.8). Bollinger

assigned a probability of existence of only 5% to the large magnitude ETSZ source. Therefore, the Bollinger (1992) source model for the SRS gave a significantly higher weight to a moderate magnitude M_{\max} for the ETSZ. The M_{\max} weighted mean for the ETSZ in his model is **M6.4**.

The USGS source model (Frankel et al. 2002) defines the ETSZ M_{\max} distribution as a single magnitude of **M7.5** with a weight of 100%. This M_{\max} includes no uncertainty in the distribution and implies that the ETSZ source zone will produce earthquakes greater than that assigned to the Charleston seismic source, which was given an M_{\max} distribution of **M6.8** to **M7.5** (Frankel et al. 2002).

In comparison, the M_{\max} distribution for EPRI ESTs range from **M4.8** to **M7.5**. The EPRI ESTs considered a broad range of M_{\max} in their incorporation of multiple expert opinions and approaches for estimating M_{\max} , as part of their effort, which would be considered a SSHAC Level 4 study. The EPRI magnitude range incorporates the USGS **M7.5**, albeit at a much lower weight. The 5% weighted **M7.8** by Bollinger (1992) slightly exceeds the EPRI range, but the **M6.3** value was given nearly the entire weight (95%) in his characterization of the ETSZ. This smaller magnitude is much closer to the mean magnitude (~**M6.2**) of the EPRI study.

The Trial Implementation Project (TIP) (Savy et al. 2002) also provided a broad M_{\max} distribution for the ETSZ. This study was designed to provide guidance in performing PSHA for nuclear plant sites, and specifically “ways to approach the issue of uncertainty in the characterization of seismic sources and in the development of ground motion models” (Savy et al. 2002). In this study, the ETSZ was characterized using multiple source zones each having a cumulative M_{\max} distribution that incorporated the opinions of five different experts. The magnitude distributions for all ETSZ source zone representations ranged from as low as **M4.5** to as high as **M7.5**, with the mode of about **M6.5** for almost each distribution (Savy et al. 2002, pages F-12 to F-19 of Appendix F). The broad distribution of the TIP study magnitude distribution for the ETSZ source zones is very similar to the EPRI distribution of **M4.8** to **M7.5**. Both of these distributions have regarded **M7.5** as the uppermost limit on M_{\max} for the ETSZ.

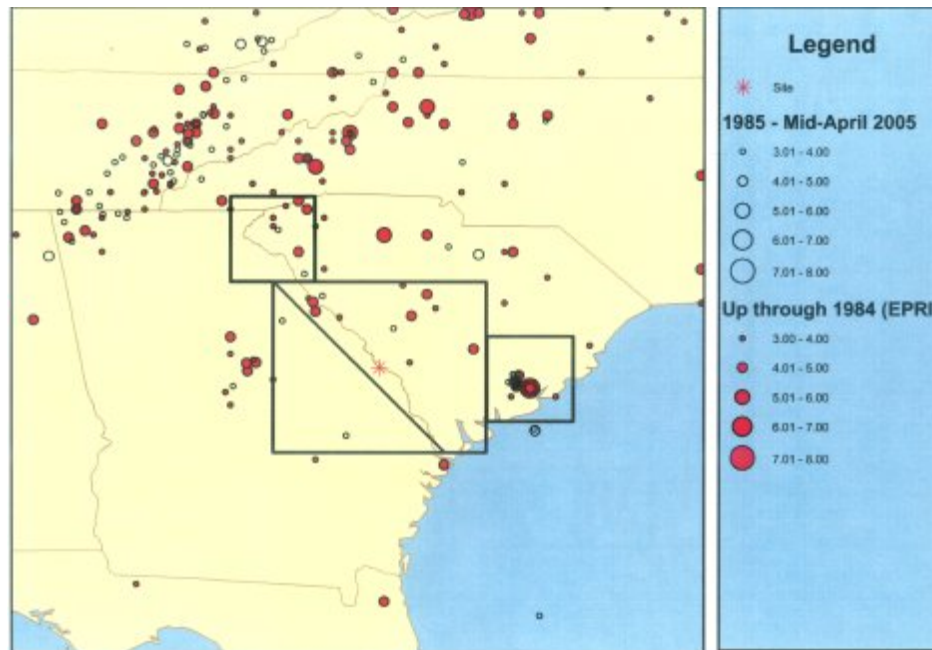
The ETSZ is characterized by abundant seismicity, but has yet to produce a recorded event greater than **M5**, which is about the minimum magnitude used to characterize seismic sources in modern PSHA studies. In our opinion, we believe that there is sufficient uncertainty in the M_{\max} potential of the ETSZ that a broad range of magnitudes is appropriate and that the EPRI model sufficiently captures the range of more recent M_{\max} distributions for this source. While the ETSZ may be capable of producing a **M7.5**, we do not believe that a weight of 0.5 to 1.0 for this magnitude represents the range of expert opinion reflected in the post-EPRI studies by Bollinger (1992) and Savy et al. (2002). The exception, of course, is the USGS model that assigns a single magnitude of **M7.5**.

The next revision to the ESP application will address as appropriate the information provided in this response.

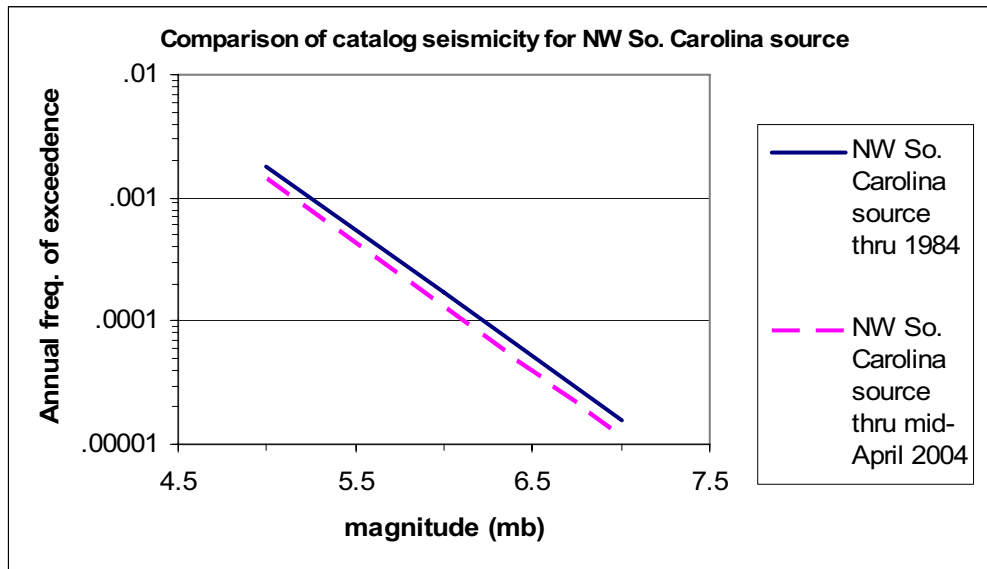
2.5.2-18 SSAR Section 2.5.2.4.2 describes the effects of the new regional earthquake catalog. Figure 2.5.2-16 shows the two areas used to examine the effect of the new seismicity information. Please provide a justification for the geometries of the two areas.

Response:

Several areas were used to examine the effect of the new regional earthquake catalog. RAI Figure 2.5.2-18A shows those regions. All four regions showed the same result, that additional seismicity from 1985 to mid-2004 does not increase estimated activity rate in the area around the Vogtle site. As an example, RAI Figure 2.5.2-18B shows the effect of additional seismicity in the square, northwest-South Carolina source shown in RAI Figure 2.5.2-18A. The estimated activity rate decreases, similar to what is shown in SSAR Figure 2.5.2-18. We conclude that any region in South Carolina that would affect the seismic hazard of Vogtle would have estimated activity rates stay constant or decrease, if the new regional earthquake catalog were added to the analysis.



RAI Figure 2.5.2-18A: Seismicity in southeastern US, showing earthquakes in the EPRI catalog (red dots) through 1984 and additional seismicity, 1985—mid April 2004 from the updated regional earthquake catalog.



RAI Figure 2.5.2-18B: Comparison of estimate activity rates for the square source in northwest South Carolina shown in RAI Figure 2.5.2-18A, for the original EPRI catalog and including the updated regional catalog.

2.5.2-19 SSAR Section 2.5.2.5.1 describes the development of the site amplification functions and the soil uniform hazard response spectra (UHRS) for the 10-4 and 10-5 hazard levels. Please provide a detailed step-by-step discussion of the methodology used to develop the site amplification functions (i.e. Steps 1 to 6 in SSAR Section 2.5.2.5.1.1) and the 10-4 and 10-5 soil UHRS. If possible, please illustrate each step with relevant data.

In addition, please discuss the following:

- a. In Step 5 of SSAR Section 2.5.2.5.1.1, what does the “envelope motion” refer to?
- b. In Step 6, please explain why either the high- or low-frequency mean amplification factor was used instead of their envelope?
- c. Step 6 states that “at some intermediate frequencies between 2 and 8 Hz, the high frequency (HF) and low frequency (LF) soil amplification factors (AF) are weighted in order to achieve a smooth transition between HF and LF spectra”. Please provide more information regarding this weighting procedure.

Response:

The six steps described in Section 2.5.2.5.1 are repeated and expanded here, to provide a more detailed description of the method used to calculate soil UHS.

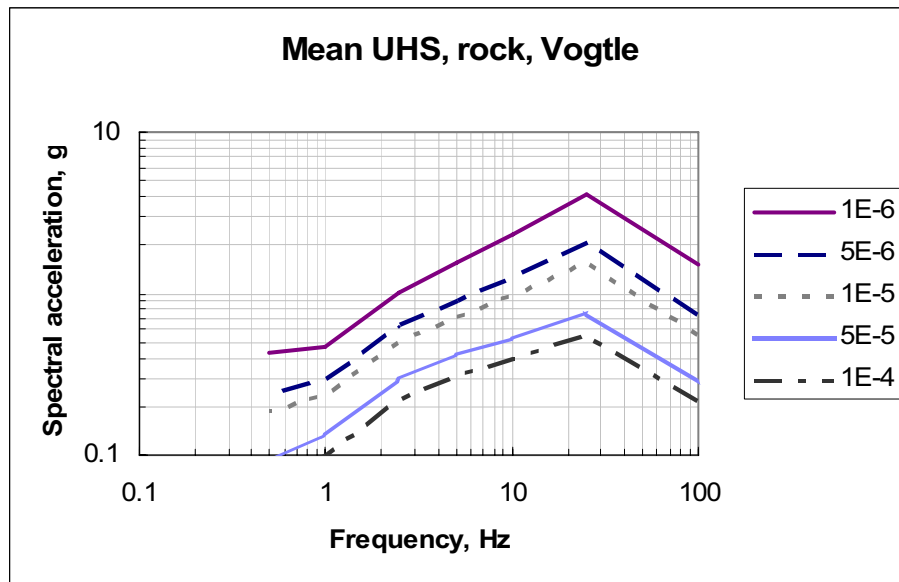
STEP 1: ROCK HAZARD

SECTION 2.5.2.5.1, STEP 1.: “The seismic hazard is calculated for hard rock conditions for the seven structural frequencies, over a range of ground motion amplitudes, resulting in a range of annual frequencies of exceedance.”

STEP 1: PSHA is performed for hard rock conditions for 7 structural frequencies to calculate the 10^{-4} , 5×10^{-5} , 10^{-5} , 5×10^{-6} , and 10^{-6} rock uniform hazard spectral [UHS] ordinates at the 7 frequencies. Values are reported numerically in SSAR Table 2.5.2-16 and graphically in SSAR Figure 2.5.2-21, repeated here:

SSAR Table 2.5.2-16 Hard Rock Mean UHS Results (in g) for VEGP ESP

Mean annual frequency of exceedance	Spectral frequency						
	PGA	25 Hz	10 Hz	5 Hz	2.5 Hz	1 Hz	0.5 Hz
10^{-4}	0.214	0.551	0.399	0.317	0.223	0.101	0.0653
5×10^{-5}	0.288	0.762	0.532	0.412	0.294	0.134	0.0924
10^{-5}	0.559	1.54	0.983	0.728	0.512	0.235	0.185
5×10^{-6}	0.747	2.06	1.28	0.914	0.635	0.294	0.241
10^{-6}	1.48	4.09	2.33	1.54	1.02	0.465	0.423



SSAR Figure 2.5.2-21 Mean Uniform Hazard Spectra, Hard Rock Conditions, for VEGP ESP

STEP 2: DEAGGREGATION

SECTION 2.5.2.5.1, STEP 2: “For ground motion amplitudes corresponding to annual frequencies of 10^{-4} , 10^{-5} , and 10^{-6} , the seismic hazard is deaggregated for high frequencies (HF) and low frequencies (LF), as described in Section 2.5.2.4.6, to determine the dominant magnitudes and distances for those amplitudes and frequencies.”

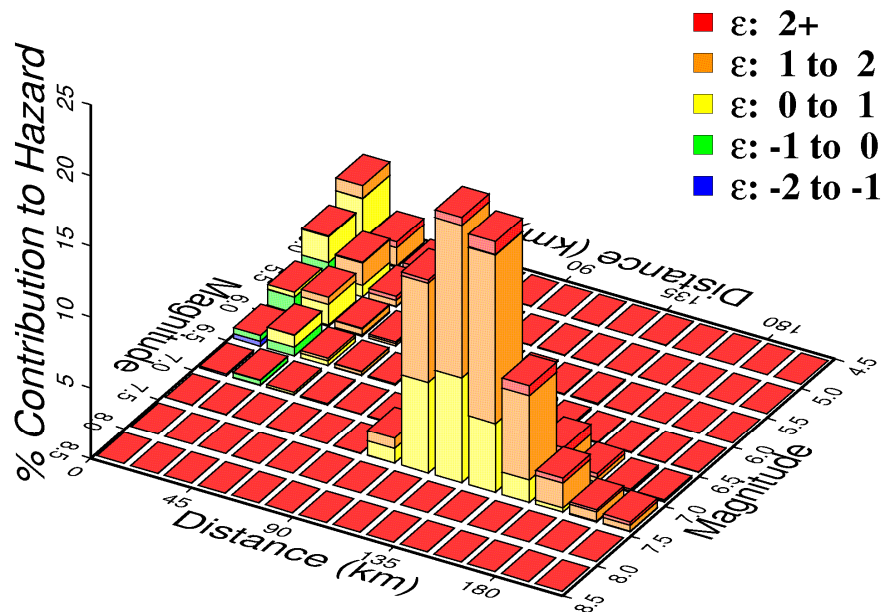
STEP 2. Using the guidance of Appendix C of Reg. Guide 1.165 [RG1.165], determine the mean magnitude M_{bar} and mean distance D_{bar} of earthquakes contributing to the hazard for ground motions with mean annual frequencies of exceedance (MAFE) of 10^{-4} , 10^{-5} , and 10^{-6} for 1 & 2.5 Hz [LF] (combined deaggregation) and for 5 & 10 Hz [HF] (combined deaggregation). These values of M_{bar} and D_{bar} are similar enough that one set of M_{bar} and D_{bar} values can be used for LF and one set can be used for HF. Results for the 3 MAFEs are shown in SSAR Table 2.5.2-17, repeated below, along with the recommended values. The recommended values were chosen to be central values that represent results for the 3 MAFEs, using 2 significant figures. SSAR Figure 2.5.2-22, also repeated below, shows that

these values of Mbar and Dbar capture the small, nearby earthquakes and large, distant earthquakes that contribute to the hazard.

SSAR Table 2.5.2-17, Computed and Recommended Mbar and Dbar Values Used for Development of High and Low Frequency Target Spectra

<i>High Frequency (5-10 Hz)</i>				
	10^{-4}	10^{-5}	10^{-6}	Recommended Values
Mbar (Mw)	5.6	5.6	5.7	5.6
Dbar (km)	17.6	11.4	9.0	12
<i>Low Frequency (1-2.5 Hz)</i>				
	10^{-4}	10^{-5}	10^{-6}	Recommended Values
Mbar (Mw)	7.2	7.2	7.2	7.2
Dbar (km)	136.5	134.3	133.0	130

High Frequency, $1.0e-4$

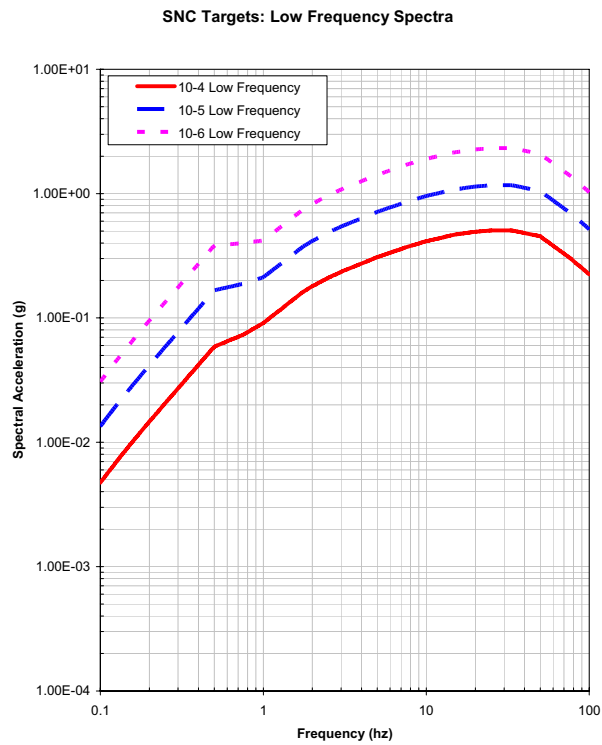
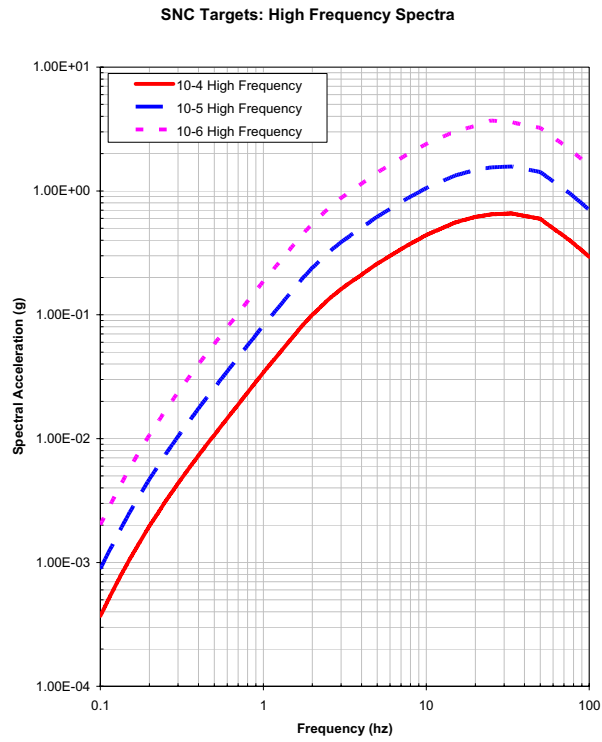


SSAR Figure 2.5.2-22 Magnitude-Distance Deaggregation for High Frequencies, 10^{-4} Mean Annual Frequency of Exceedance

STEP 3: ROCK SPECTRA

SECTION 2.5.2.5.1, STEP 3.: “HF hard rock spectra are developed to represent earthquakes dominating the 5-10 Hz ground motions, and LF hard rock spectra are developed to represent earthquakes dominating the 1-2.5 Hz ground motions. These hard rock spectra represent the mean magnitude and distance of earthquakes that dominate the seismic hazard for those structural frequencies.”

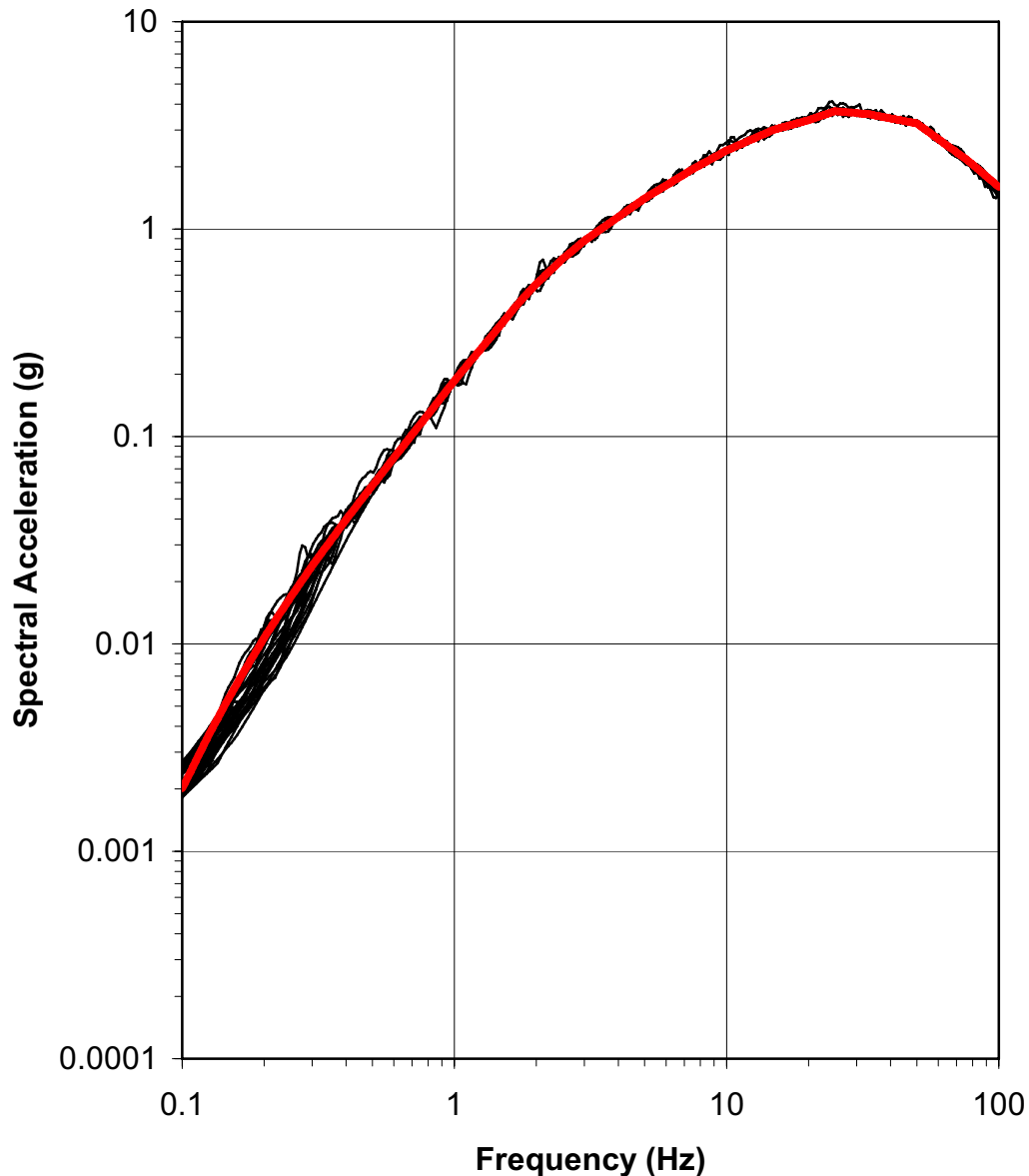
STEP 3A: Use the Mbar and Dbar values from Step 2 to generate HF and LF hard rock spectral shapes using the recommended shapes in NUREG/CR-6728. Following Reg. Guide 1.165, scale the HF spectral shapes to match the 7.5 Hz spectral acceleration equal to the linear average of the spectral accelerations at 5 and 10 Hz for each of the three MAFEs. Similarly, scale the LF spectral shapes to match the 1.75 Hz spectral acceleration equal to the linear average of the spectral accelerations at 1 and 2.5 Hz for each of the three annual frequency levels. This step results in smooth spectra for each of the three MAFEs. As discussed in SSAR Section 2.5.2.5.1.3, an additional NUREG/CR-6728 requirement that the envelop of the scaled HF and LF target spectra for a given annual probability level be no less than 90 percent of the UHS was applied. The spectra are illustrated in SSAR Figure 2.5.2-35, repeated below.



SSAR Figure 2.5.2-35 High and Low-Frequency Target Spectra for the Three Annual Probability Levels of 10^{-4} , 10^{-5} , and 10^{-6}

STEP 3B. The spectra from Step 3A are used as target spectra to spectrally match 30 time histories for each frequency band [HF and LF] and each MAFE [10^{-4} , 10^{-5} , and 10^{-6}], resulting in 180 time histories. This step is illustrated for HF and a MAFE of 10^{-6} in SSAR Figure 2.5.2-36a, repeated below.

Spectral-Matched Time History Spectra: RP6HF



SSAR Figure 2.5.2-36a, High Frequency (10^{-6}) Match for the 30 Time Histories

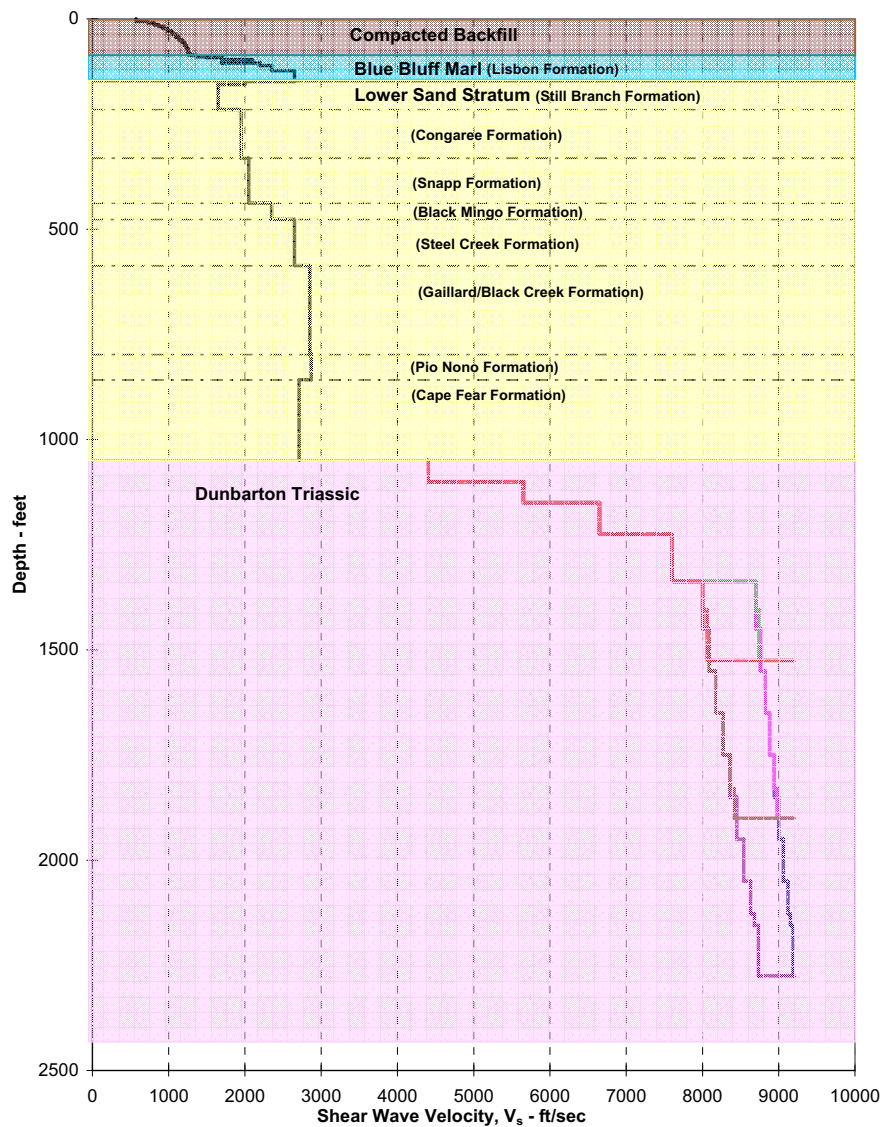
Note: Heavy red line is the target spectrum and thin black lines are the individual matches.

STEP 4: CALCULATE SOIL AMPLIFICATION

SECTION 2.5.2.5.1, STEP 4. “The rock and soil column is modeled, and soil amplitudes are calculated at the control point elevation for input hard rock motions corresponding to frequencies of exceedance of

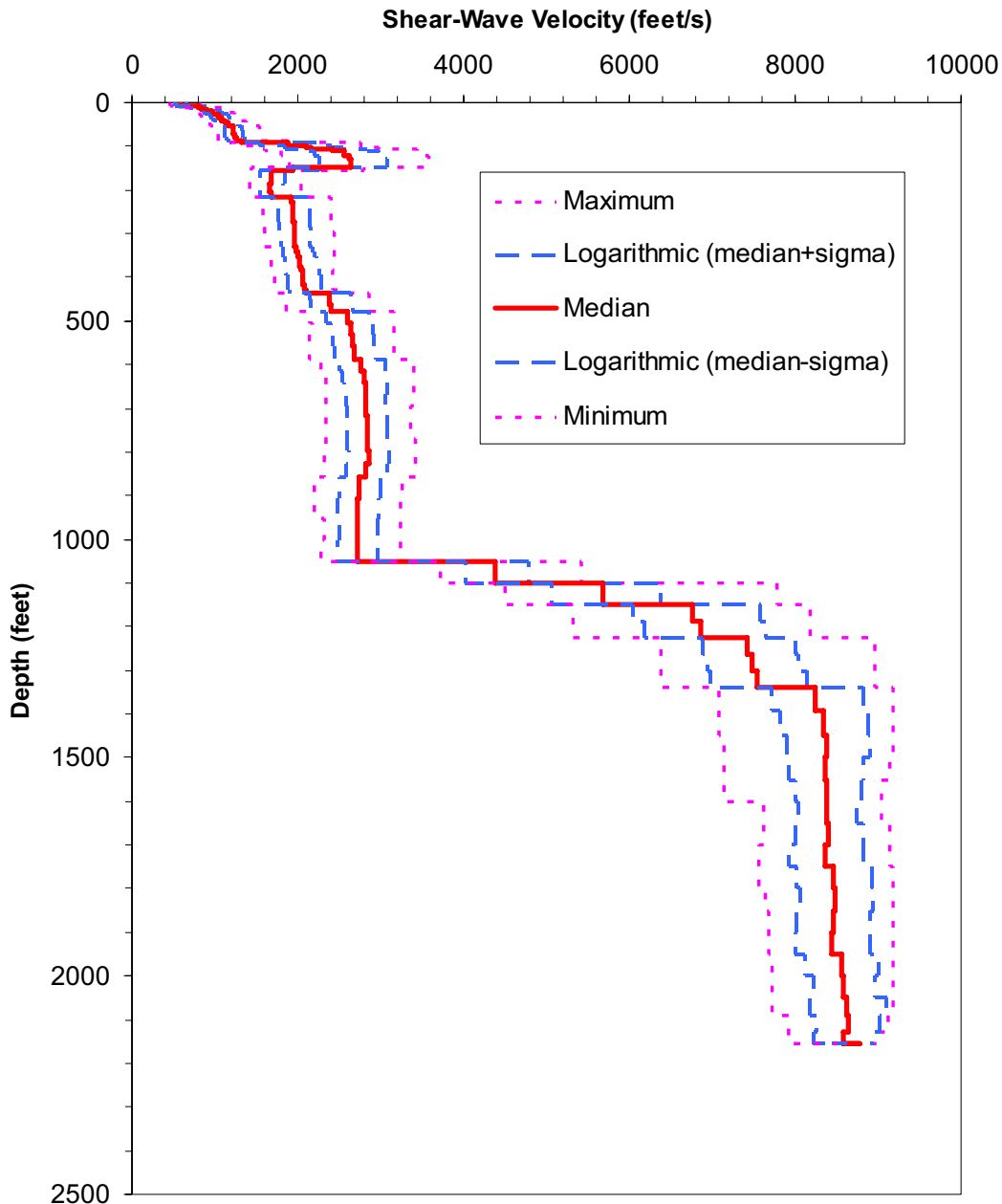
10^{-4} , 10^{-5} , and 10^{-6} . These calculations are made separately for ground motions dominating the HF hard rock motion and the LF hard rock motion, and the input motions have a spectrum determined by the HF or LF hard rock spectral shape, as appropriate. Multiple hard rock motions are used, and multiple soil column properties are used, so that the mean soil amplitudes can be determined accurately.”

STEP 4A: Mean soil/rock column characteristics are determined using both EPRI and SRS material curves. These soil/rock characteristics are shear-wave velocity, stiffness, and damping (the latter two are specified for each layer as a function of soil strain). The soil/rock column is modeled to a depth at which the rock shear-wave velocity equals 9200 fps. SSAR Figure 2.5.4-7 below illustrates the low strain base case shear-wave velocity profiles vs. depth.



SSAR Figure 2.5.4-7 – Shear Wave Velocity for SHAKE Analysis

STEP 4B: Soil and rock column characteristics (shear-wave velocities vs. depth, stiffness, and damping vs. soil strain for each layer) are randomized accounting for estimated uncertainties in each characteristic and for correlation in characteristics among adjacent layers. Using simulation, 60 soil/rock column characteristics are generated for the EPRI mean material curves, and 60 characteristics are generated for the SRS mean material curves. SSAR Figure 2.5.2-34, repeated below, illustrates the median, median \pm sigma, and maximum/minimum shear-wave velocities vs. depth for the simulated shear-wave velocities.



SSAR Figure 2.5.2-34 Summary Statistics Calculated from the 60 Shear-Wave Velocity Profiles

Note: Statistics do not include the velocities on the crystalline bedrock.

STEP 4C: The dynamic site response to shaking is calculated using software SHAKE for each of the spectrally matched time histories from Step 3B, and each set of soil characteristics from step 4B. SHAKE analyses were conducted for 300 structural frequencies between 0.1 Hz and 100 Hz. For the SHAKE analyses, each of the 30 time histories from Step 3B is randomly paired with 2 of the randomized soil/rock columns, to achieve a random group of 60 input motions and soil/rock characteristics. This information is provided in SSAR Table 2.5.2-19. Each SHAKE analysis produces amplification results at the control point horizon.

This step, therefore, consists of 720 SHAKE analyses, as follows:

Ground motion levels [10^{-4} , 10^{-5} , and 10^{-6}]	3
Frequency bands [HF and LF target spectra]	× 2
Material curve models [EPRI and SRS]	× 2
60 randomized soil/rock columns	× <u>60</u>
Total SHAKE analyses:	720

For the SHAKE analyses, each of the 30 time histories from Step 3B is randomly paired with 2 of the randomized soil/rock columns, to achieve a random group of 60 input motions and soil/rock characteristics. Each SHAKE analysis produces amplification results at the 3 depths.

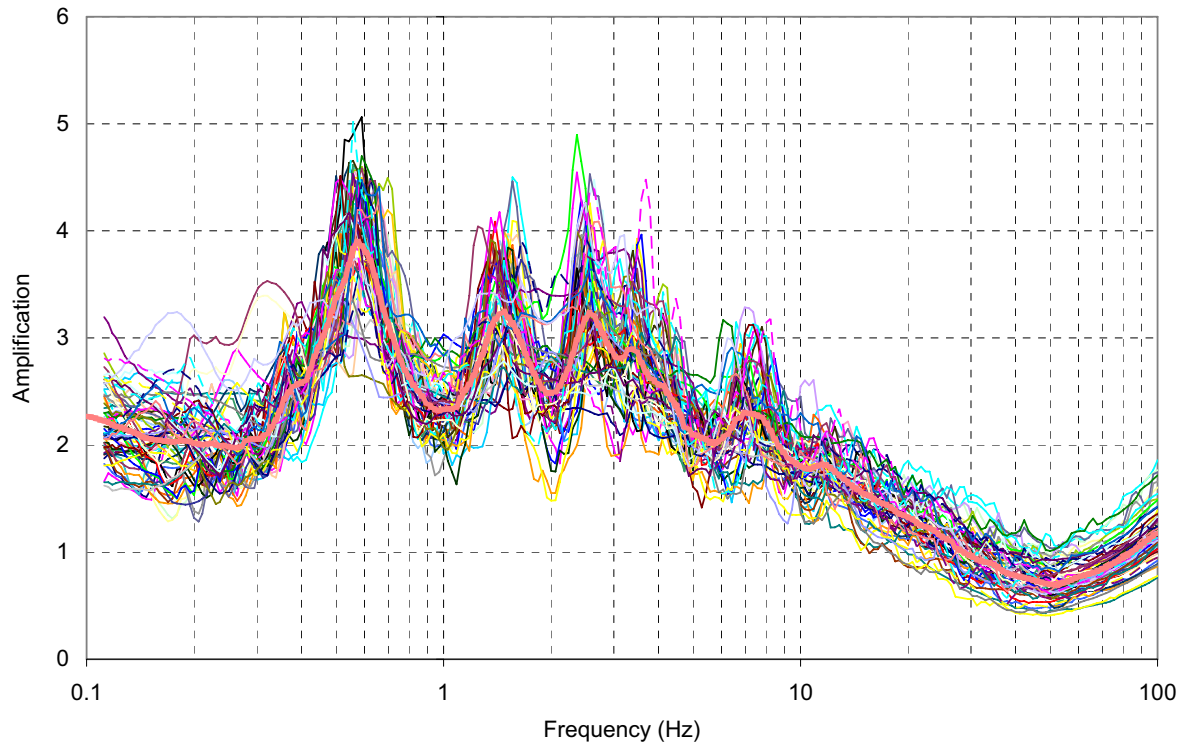
STEP 5: SOIL AMPLIFICATION FACTORS

SSAR 2.5.2.5.1, STEP 5: “The soil amplification factors (AFs) are developed at 300 frequencies using analyses described in this section based on the HF and LF hard rock spectral shapes. The AFs represent the mean spectral acceleration (SA) at the control point, divided by input SA at hard rock, at each frequency. At each frequency, the soil envelope motion [at the control point horizon (86’ depth)] is determined. This is the motion (HF or LF) that gives the higher mean soil motion, for that structural frequency and MAFE. At frequencies above 8 Hz, this is always the HF motion. At frequencies below 2 Hz, this is always the LF motion. At intermediate frequencies, the envelope motion depends on the frequency and the MAFE.”

STEP 5A: The mean and standard deviation of amplification factors [AFs] (soil SA divided by rock SA at each of the 300 structural frequencies) is calculated using the 60 randomized sets of soil/rock characteristics. (Means and standard deviations are calculated logarithmically.) This results in 12 sets of mean AFs (one set being for the 300 structural frequencies), as follows:

Ground motion levels [10^{-4} , 10^{-5} , and 10^{-6}]	3
Frequency bands [HF and LF target spectra]	× 2
Material curve models [EPRI and SRS]	× 2
Depth horizons [86 feet]	× <u>1</u>
Total sets of mean AFs:	12

SSAR Figure 2.5.2-37, repeated below, illustrates the 60 individual AFs and the mean AF across the frequency range of 0.1 Hz to 100 Hz, for the 10^{-4} MAFE, HF input, EPRI mean material curves, and 86’ depth.



SSAR Figure 2.5.2-37 Typical Results of Spectral Amplification at 86-ft Depth (Top of Blue Bluff Marl) Using EPRI Degradation Curves for High Frequency Time Histories of 10^{-4} MAFE Input Motion Level

STEP 5B: The mean AFs for the EPRI and SRS material curves are equally weighted, to give 6 mean AFs across the frequency range 0.1 Hz to 100 Hz, for the control point horizon. These 6 mean AFs correspond to the 3 ground motion levels and to the HF and LF input motions.

STEP 5C: The controlling HF or LF input motion is determined over the frequency range 0.1 Hz to 100 Hz for each MAFE, by examining the envelope of soil response at the control point location (86' depth) due to the HF and LF rock motion. Note from Figure 2.5.2-35 (in the SSAR and above) that, at high frequencies, the HF rock input motion exceeds the LF rock input motion. At low frequencies, the reverse is true. This means that the HF input rock motion will control the high frequency soil responses (above 8 Hz) and the LF input rock motion will control the low frequency soil responses (below 2 Hz). In between, the controlling motion, which is the maximum soil response, depends on the MAFE and the frequency. This step results in one set of mean AFs (across the frequency range 0.1 Hz to 100 Hz) for each MAFE.

STEP 6: CALCULATE SOIL UHS

SSAR Step 6: "The uniform hazard response spectra at MAFEs of 10^{-4} and 10^{-5} at the control point location are calculated as follows. Starting from the 10^{-4} and 10^{-5} SA hard rock values (from the hazard calculations described in 2.5.2.4) at the seven structural frequencies, interpolation is performed between those SA values to obtain 10^{-4} and 10^{-5} SA values at the 300 structural frequencies using the HF and LF spectral shapes for hard rock. The choice of HF or LF is based on the envelope motion determined in the previous step. The UHS for 10^{-4} at the control point location is calculated by multiplying the hard rock 10^{-4} SA values at the 300 frequencies by the mean AFs for 10^{-4} from step 5, again using the HF or LF mean AF corresponding to the envelope motion. (At some intermediate frequencies between 2 and 8 Hz,

the HF and LF AFs are weighted in order to achieve a smooth transition between HF and LF spectra.) The UHS for 10^{-5} is calculated in a similar way, using the 10^{-5} rock SA values and the 10^{-5} AFs.”

STEP 6A: Similar to Step 3A, use rock spectral shapes recommended in NUREG/CR-6728 to develop rock spectra for the HF and LF controlling earthquakes. In this step, however, the rock spectra are adjusted to equal the 7 PSHA structural frequencies at the 3 MAFEs of interest (10^{-4} , 10^{-5} , and 10^{-6}). The spectral shapes are used to interpolate between these frequencies, and to extrapolate below 0.5 Hz. Because both the HF and LF spectra are constrained to equal the 7 PSHA structural frequencies at the 3 MAFEs of interest, the resulting HF and LF spectral shapes are similar, particularly at high frequencies. A single continuous rock spectrum is derived from 0.1 Hz to 100 Hz that equals the 7 PSHA structural frequencies at the 3 MAFEs of interest and is the envelope of the HF and LF spectra that conform to spectral amplitudes for the 7 PSHA structural frequencies. Constraining the rock spectra in this step to equal the amplitudes at the 7 structural frequencies at which the PSHA was calculated ensures that the proper rock motion at each structural frequency will be used to calculate the soil amplitude, for that MAFE.

STEP 6B: Multiply the rock spectra for each MAFE from Step 6A, times the mean AFs from Step 5C, at each frequency in the range 0.1 Hz to 100 Hz, to calculate soil UHS at the 86' depth for each MAFE. At frequencies above 8 Hz, this spectrum is controlled by the HF AFs. At frequencies below 2 Hz, this spectrum is controlled by the LF AFs. At intermediate frequencies interpolation is used to achieve a smooth transition between the HF and LF parts of the spectrum.

SUMMARY

The above 6 steps summarize the calculation of soil UHS for each depth. These soil spectra are used to develop the depth-specific DRS.

2.5.2-20 SSAR Section 2.5.2.5.1.3 describes the development of low- and high- frequency target spectra using the average of the single and double corner source models from NUREG/CR-6728. Please explain why the 2004 EPRI (EPRI 1009684 2004) ground motion models were not used instead.

Response:

The 2004 EPRI ground motion report (EPRI 1009684) gives equations to estimate spectral acceleration at 7 structural frequencies (100, 25, 10, 5, 2.5, 1, and 0.5 Hz). To properly represent rock motion for input to a site response analysis, it is necessary to interpolate between these 7 structural frequencies to obtain a realistic spectral shape, rather than using linear interpolation. For this task, NUREG/CR-6728 was used, because one of its goals was specifically to develop realistic spectral shapes for the eastern US to use in earthquake ground motion analyses.

2.5.2-21 SSAR Table 2.5.2-17 and Section 2.5.2.5.1.3 provides the computed and recommended Mbar and Dbar values used for the development of the high- and low-frequency target response spectra. Please explain how the “recommended” Dbar and Mbar values were calculated.

Response:

Mean magnitude (Mbar) and distance (Dbar) values were computed for three annual probability levels: 1×10^{-4} , 1×10^{-5} , and 1×10^{-6} based on the seismic hazard curves for both the high- and low-frequency cases. Table 2.5.2-17 of the SSAR lists these values along with the recommended magnitude and distance values used in the analysis. These recommended values were selected such that they approximately represent the

AR-07-0801
Enclosure 1
RAI Response

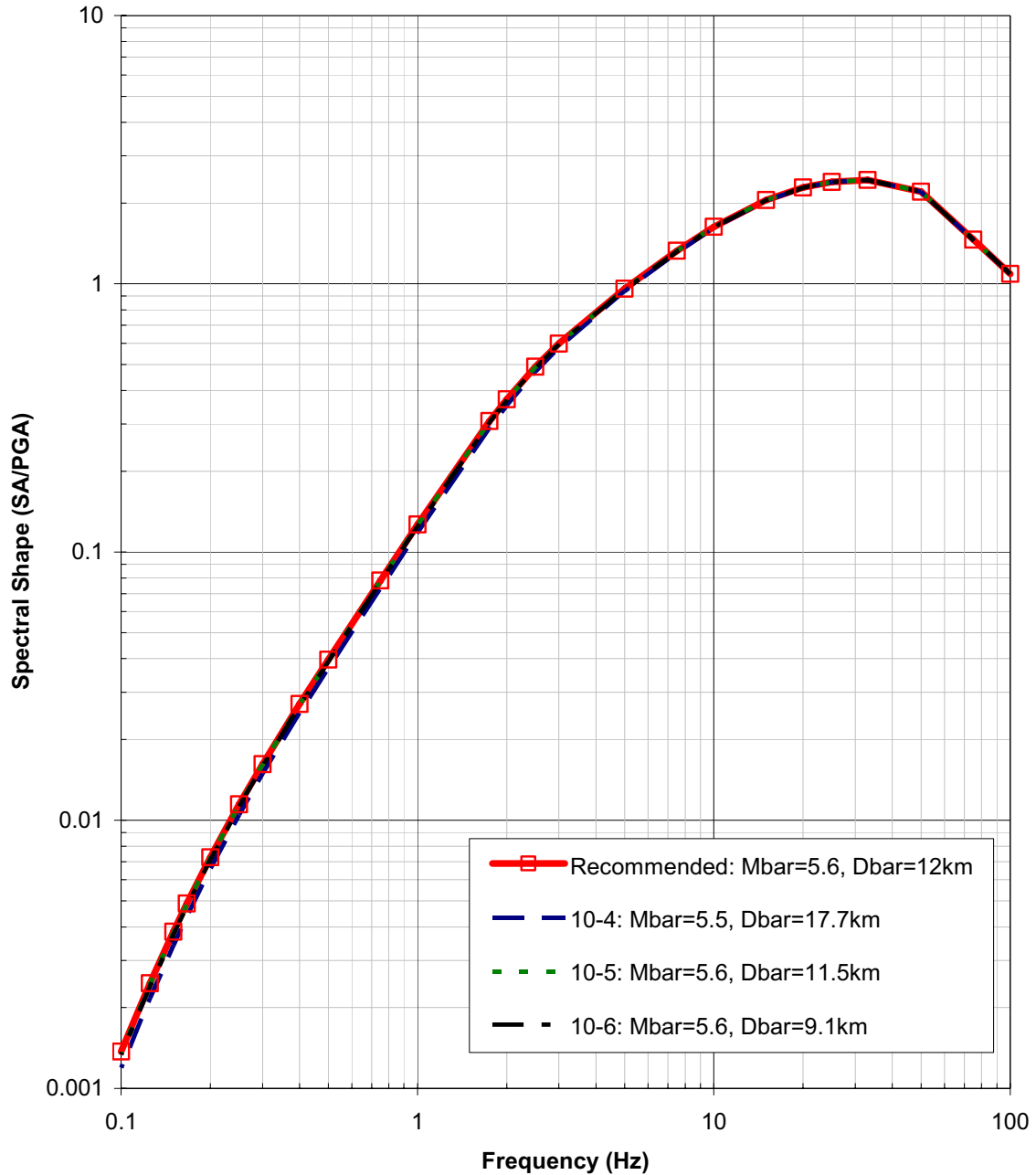
range in Mbar and Dbar values computed for the three annual probability levels for both the high- and low-frequency cases based on the bi-modal distribution of the deaggregation. These recommended values were not computed based on a statistical average or otherwise from the explicit values for each of the three annual probability levels. For the low frequency case, the recommended distance value was assigned of distance of 130 km based on the source to site distance for the Charleston source. For the high frequency case, the recommended distance is approximately equal to the log-average of the three computed values rounded to the nearest km. The recommended magnitude values for both the high- and low-frequency cases is equal to the linear average of the three magnitude values rounded to the nearest tenth of a magnitude unit.

These recommended Mbar and Dbar values were used to simplify the analysis, rather than the computed values at the three annual probability levels, for the development of the corresponding target spectra and to a lesser extent in the time history selection procedure for the site response analysis. RAI Figure 2.5.2-21a shows the difference in spectral shapes for the high-frequency case using the recommended magnitude and distance values and the computed magnitude and distance values for the three annual probability levels. The same comparison is presented in RAI Figure 2.5.21b for the low-frequency case. Based on these comparison plots, the use of the recommended magnitude and distance values in place of the computed magnitude and distance values for each of the three annual probability levels would not significantly change the results of the site response analysis.

The recommended magnitude and distance values were also used as guides in selecting the seed input time histories for the spectral matching analysis associated with the site response analysis. Based on the selection of time histories which fall within a given magnitude and distance range and the similarity between the recommended and computed magnitude and distance values, the use of the recommended values would not change the selected time histories used in the site response analysis.

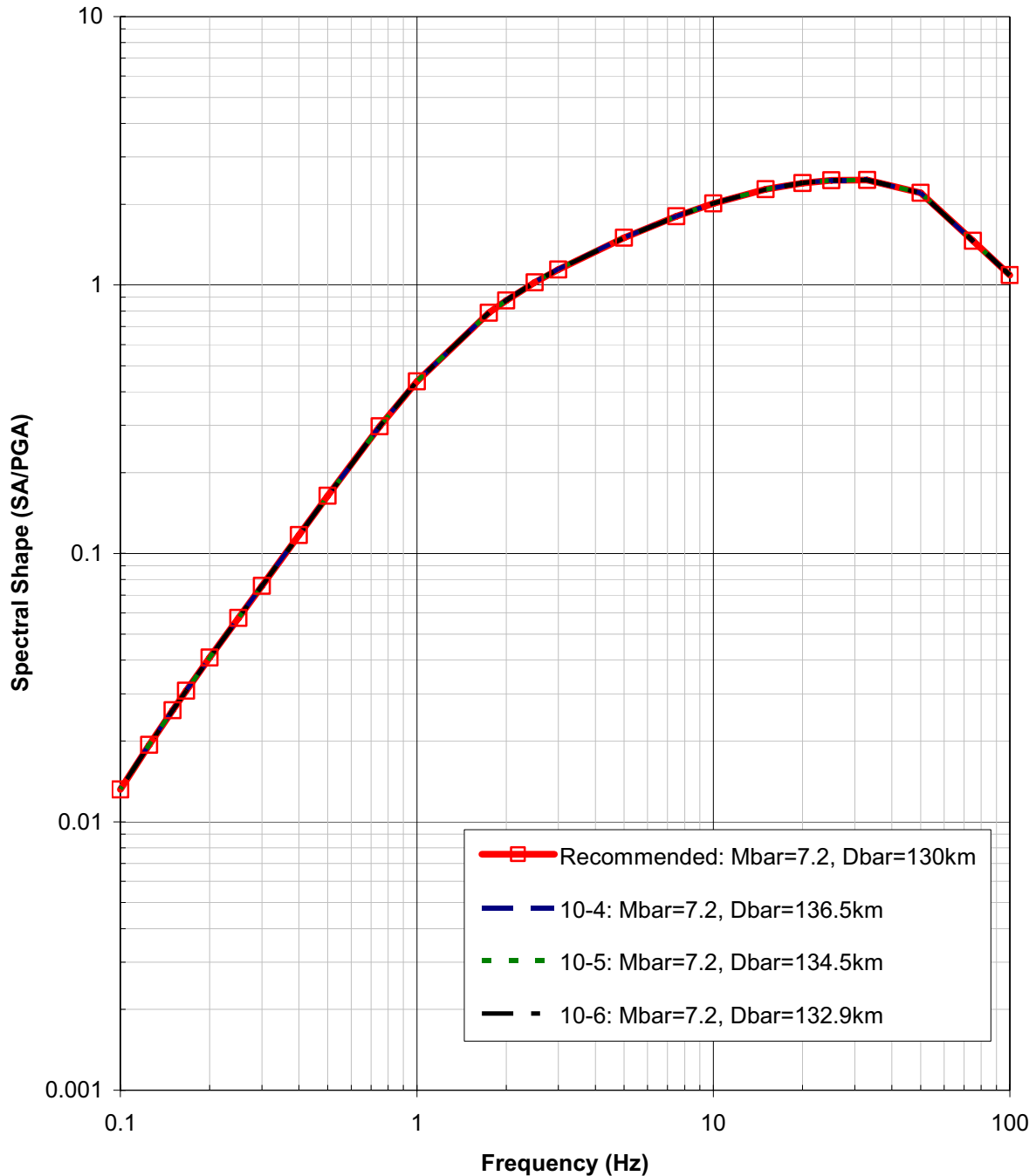
The next revision to the ESP application will address as appropriate the information provided in this response.

SNC (High Frequency): NUREG CR-6728 Spectral Shapes



RAI Figure 2.5.2-21a Comparison between high-frequency spectral shapes using the recommended magnitude and distance values and the computed magnitude and distance values for the three annual probability levels of 1×10^{-4} , 1×10^{-5} , and 1×10^{-6} .

SNC (Low Frequency): NUREG CR-6728 Spectral Shapes



RAI Figure 2.5.2-21b. Comparison between low-frequency spectral shapes using the recommended magnitude and distance values and the computed magnitude and distance values for the three annual probability levels of 1×10^{-4} , 1×10^{-5} , and 1×10^{-6} .

2.5.2-22 SSAR Section 2.5.2.5.1.4 describes the spectral matching of the selected seed time histories to the target response spectra and states that the “spectral matching criteria given in NUREG/CR-6728 (McGuire et al. 2001) were used to check the average spectrum from the 30 time histories for a given frequency range (high- or low-frequency) and annual probability level. This is the recommended procedure in NUREG/CR-6728 (McGuire et al. 2001) when multiple time histories are being generated and used.” In addition, Section 2.5.2.5.1.5 states that “Each of the 60 randomized soil profiles were paired with 30 seed time histories (each time history was applied to two of the randomized soil profiles)”.

Please provide a justification for not using the criteria provided in NUREG/CR-6728 to check each individual time history against the target spectrum.

Response:

For the site response analysis a total of 30 acceleration horizontal time histories were modified to be spectrum compatible to given target spectrum. Target spectra were developed for both the high- and low-frequency cases at each of the three annual probability levels: 1×10^{-4} , 1×10^{-5} , and 1×10^{-6} . This resulted in a total of 180 spectrum compatible acceleration time histories for the site response analysis. For a given suite of 30 time histories, the spectral matching criteria given in NUREG CR-6728 were followed. Specifically, item (e) of the general criteria recommended for evaluating the adequacy of the artificially developed ground motions states,

“(e) The computed 5% damped response spectrum of the artificial ground motion (if one motion is used for analysis) or the mean of the 5% damped response spectra (if a suite of motion is used for the analysis) should not exceed the target spectrum at any frequency by more than 30% (a factor of 1.3) in the frequency range between 0.2 Hz and 25 Hz.”

The average site response amplification factors were developed for each given suite of 30 input spectrum compatible time histories (i.e., given high- or low-frequency case for a given annual probability level) and the 60 randomized soil profiles. Based on this use of multiple time histories matched to the same target spectrum for the site response analysis and the criteria given in NUREG CR-6728 and listed above, the compliance between the average response spectrum from a given set of 30 input spectrum compatible time histories and the respective target spectrum was checked rather than the individual 30 spectrum compatible time histories to the target spectrum.

The next revision to the ESP application will address as appropriate the information provided in this response.

2.5.2-23 SSAR Section 2.5.2.5.1.5 describes the results of the site response calculations for the ESP site. Please discuss the results of site response calculations in terms of the following:

- a. The effects of the six alternative site response profiles in terms of the different depths to the top of the Paleozoic crystalline rocks.**
- b. The possible effects of the Pen Branch fault zone (i.e. as a low velocity zone or weak zone).**
- c. The effects of the low velocity zones within the Blue Bluff Marl and Lower Sand Stratum.**

In addition, please justify the adequacy of using an equivalent-linear approach rather than a nonlinear approach to model site response at the ESP site.

Response:

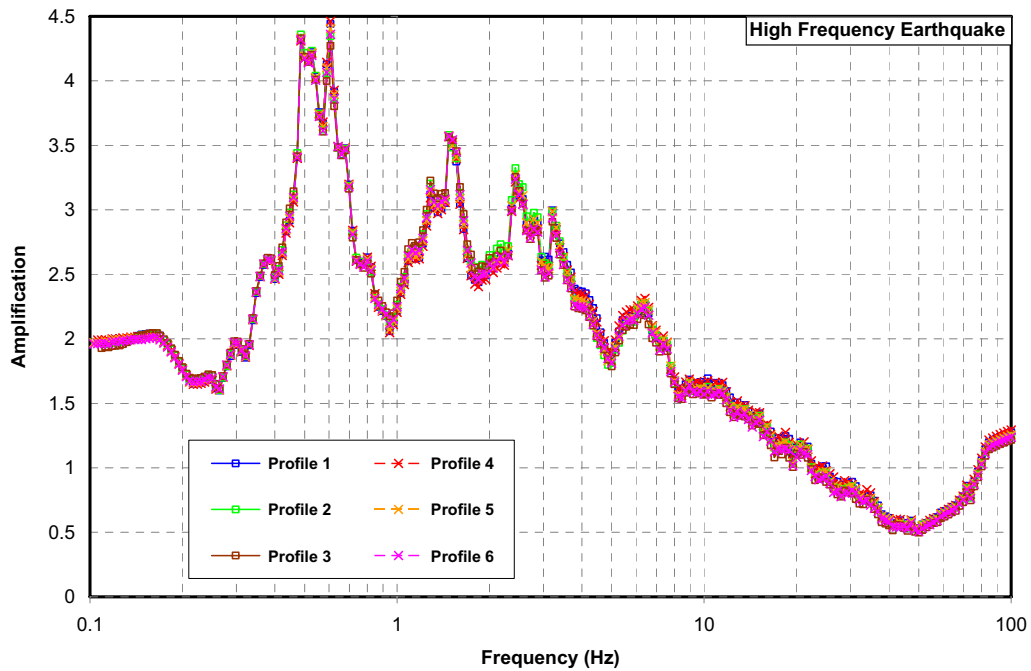
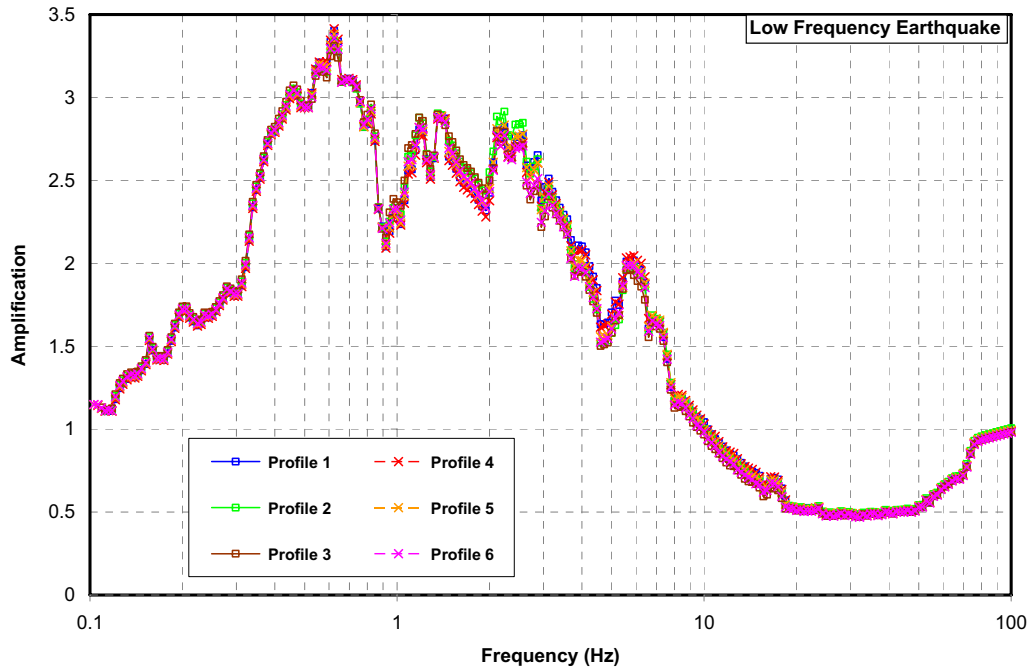
The site response analyses of the ESP site used six base profiles to represent the properties of the rock strata located below depth of 1049 ft. RAI Table 2.5.2-23A below presents the rock shear velocity profiles:

RAI Table 2.5.2-23A. ESP Site Base Profiles - Rock Shear Velocities

Top of Layer Depth (ft)	Vs (fps)		Top of Layer Depth (ft)	Vs (fps)		Top of Layer Depth (ft)	Vs (fps)	
	Prof. 1	Prof. 4		Prof. 2	Prof. 5		Prof. 3	Prof. 6
1049	4400	4400	1049	4400	4400	1049	4400	4400
1100	5650	5650	1100	5650	5650	1100	5650	5650
1150	6650	6650	1150	6650	6650	1150	6650	6650
1225	7600	7600	1225	7600	7600	1225	7600	7600
1338	8000	8700	1338	8000	8700	1338	8000	8700
1405	8059	8739	1450	8090	8760	1450	8090	8760
1525	9200	9200	1550	8180	8820	1550	8180	8820
			1650	8270	8880	1650	8270	8880
			1750	8360	8940	1750	8360	8940
			1830	8414	8976	1850	8450	9000
			1900	9200	9200	1950	8540	9060
						2050	8630	9120
						2128	8679.5	9153
						2155	8733.5	9189
						2275	9200	9200

This table is similar to SSAR Table 2.5.4-11 Part B. The profiles are grouped in three pairs with each pair of profiles having the crystalline rock at different depth (1525 ft for profiles 1 and 4, 1900 ft for profiles 2 and 5 and 2275 ft for profiles 3 and 6).

Two acceleration time histories were developed compatible with the high frequency (HF) (5-10 Hz) and low frequency (LF) (1-2.5Hz) target spectra at 1×10^{-5} probability level. SHAKE analyses were performed where the acceleration time histories were applied as outcrop object motion at the top of the crystalline bedrock. RAI Figure 2.5.2-23A compares the results of the SHAKE analyses of the six base profiles for the 5% damping acceleration response spectra (ARS) amplifications at the top of the Blue Marl at 86 ft depth. The small difference in the ARS amplifications indicate that the effect of the depth of the crystalline rock on the site response at 86 ft depth horizon where the SSE design motion is defined is relatively small, particularly in comparison to the variability of total [soil and rock] site response when soil/rock column model randomization and multiple time histories are considered (see SSAR Figure 2.5.2-37).



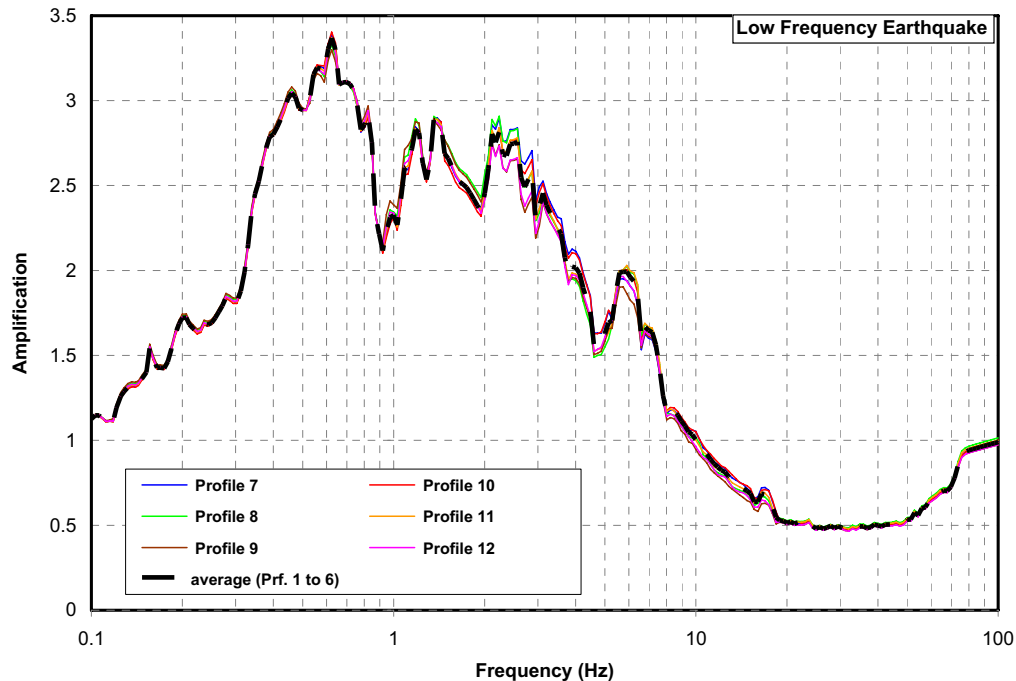
RAI Figure 2.5.2-23A. ESP Base Profiles – 5% Damping ARS Amplifications at 86 ft Depth

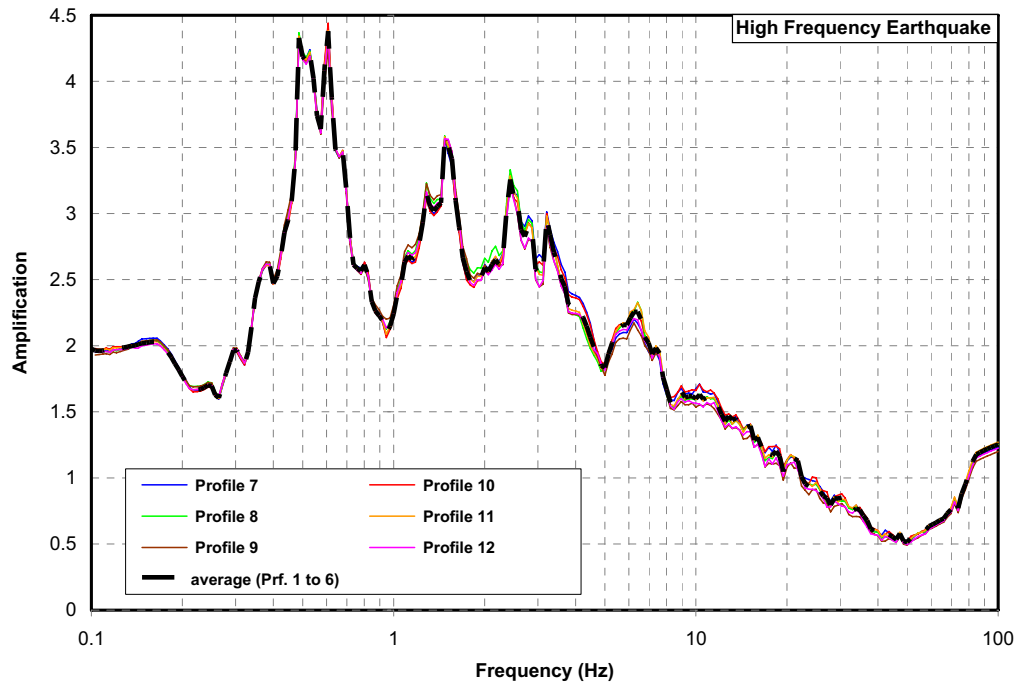
The rock shear velocities of the six base profiles in RAI Table 2.5.2-23 were modified to include the low velocity zone as listed in RAI Table 2.5.2-23B. Shake analyses were performed using the LF and HF acceleration time histories in order to calculate ARS amplifications at 86 ft depth where the SSE motion is defined.

RAI Table 2.5.2-23B. Rock Shear Velocities of the ESP Site Profiles with Low Velocity Zone -

Top of Layer Depth (ft)	Vs (fps)		Top of Layer Depth (ft)	Vs (fps)		Top of Layer Depth (ft)	Vs (fps)	
	Prof. 7	Prof. 10		Prof. 8	Prof. 11		Prof. 9	Prof. 12
1049	4400	4400	1049	4400	4400	1049	4400	4400
1100	5650	5650	1100	5650	5650	1100	5650	5650
1150	6650	6650	1150	6650	6650	1150	6650	6650
1225	7600	7600	1225	7600	7600	1225	7600	7600
1338	8000	8700	1338	8000	8700	1338	8000	8700
1405	7005	7703	1450	8090	8760	1450	8090	8760
1525	9200	9200	1550	8180	8820	1550	8180	8820
			1650	8270	8880	1650	8270	8880
			1740	8342	8928	1750	8360	8940
			1780	7342	7928	1850	8450	9000
			1900	9200	9200	1950	8540	9060
						2050	8630	9120
						2128	8679.5	9153
						2155	7679.5	8153
						2275	9200	9200

RAI Figure 2.5.2-23B shows the 5% damping ARS amplifications results at 86 ft depth obtained from the analyses of low velocity profiles 7 to 12. These ARS amplifications are compared with the log-average of the ARS amplifications obtained from the analyses of the base ESP profiles shown in RAI Figure 2.5.2-23. The comparison indicates that effects of the Pen Branch fault zone (i.e. as a low velocity zone) on the response of the site at the two SSE horizons are small.





RAI Figure 2.5.2-23B Low Velocity Profiles – 5% Damping ARS Amplifications at 86 ft Depth

The base case shear wave velocity profile is shown on SSAR Figure 2.5.4-7 and is summarized on SSAR Table 2.5.4-11. The trend is for the shear wave velocity to gradually increase with depth within the Blue Bluff Marl. However, a 3-ft thick zone of lower shear wave velocity was encountered in the Blue Bluff Marl between depths of 102 and 105 ft. The shear wave velocity in the Lower Sand Stratum shows an initial trend of decreasing with depth immediately beneath the Blue Bluff Marl. The shear wave velocity reaches its lowest values in the depth range of 156 to 216 ft, and then resumes the trend of increasing with depth. The low velocity zones in the Blue Bluff Marl and in the Lower Sand Stratum were incorporated in the site response calculations, i.e., the site response calculation results inherently reflect the inclusion of these low velocity zones. The calculations were performed using the base case shear wave velocity profile that is based on field measurements, and randomized profiles.

RAI Table 2.5.2-23C summarizes the results for the maximum soil strains obtained from the SHAKE analyses of the randomized profiles of ESP site. The table shows that the maximum soil strain remained below 0.6%. The equivalent linear approach is adequate for this low level of soil strain.

RAI Table 2.5.2-23C, SHAKE Analyses of Randomized Profiles – Maximum Soil Strains

Earthquake Probability Level	EPRI Randomized Profiles		SRS Randomized Profiles	
	LF Earthq.	HF Earthq.	LF Earthq.	HF Earthq.
10 ⁻⁴	0.078%	0.067%	0.082%	0.068%
10 ⁻⁵	0.592%	0.300%	0.287%	0.353%

The next revision to the ESP application will address as appropriate the information provided in this response.

2.5.2-24 SSAR Sections 2.5.2.7.1.1 to 2.5.2.7.1.3 describe the development of vertical-to-horizontal response spectral (V/H) ratios based on the results of NUREG/CR-6728 and Lee (2001).

- a. Please justify your rationale for assigning the approximate weights of 1:3 to the respective “near” and “far” estimates of V/HCEUS, Soil.**
- b. Please discuss the similarities and differences between the site-specific soil profile used by Lee (2001) and the Vogtle ESP site response profile.**
- c. Please justify in greater detail your rationale for the relative weights assigned to the NUREG/CR-6728 and Lee (2001) results and the final smoothing.**

In addition, SSAR Section 2.5.2.7.1.3 states that “both results give minimum V/H values, particularly in the lower frequencies, which appear lower than engineering judgment may suggest acceptable in the current state-of-knowledge”. Please explain the meaning of this statement in greater detail and its implication for the final ESP site V/H ratios.

Response:

While Reg. Guide 1.60 presents a fixed functional relationship for V/H – basically, 1.0 for high frequencies and 2/3 for low frequencies – it is recognized in the seismic ground motion community of experts (see EPRI, 1993, or McGuire and others, 2001) that V/H varies with magnitude, distance, site conditions, and tectonic environment [e.g., western US vs. central and eastern US]. This is discussed in SSAR Section 2.5.2.7.1. The SSAR attempts to consider these variables in establishing a V/H that considers some degree of Vogtle site-specificity.

In the development of the horizontal ground motions from the PSHA, the results of hazard deaggregations are presented that indicate the distribution of hazard contribution by magnitude and distance for different frequencies and hazard levels. From SSAR Figures 2.5.2-22 through 2.5.2-27 it can be seen that the “near” and “far” modes correspond to smaller magnitude and larger magnitude events, respectively. Consistent with the dominant seismic events considered for the site response analysis – see SSAR Section 2.5.2.5.1.3 – a “near” event of magnitude M5.6 at 12 km and a “far” event of M7.2 at 130 km are assumed to be reasonable mean dominant events contributing to an estimate of V/H. As V/H varies by magnitude and distance, it is desirable to estimate the relative contribution of these two representative events to the development of V/H by ascribing weights to the “near” and “far” events.

SSAR Figure 2.5.2-30 presents a different view of high-frequency deaggregation – contribution over magnitude has been summed, and the explicit dependence on magnitude is lost. However, from the other figures of magnitude-distance deaggregation, it is known that the distinct bimodal character of the “near” [i.e., <20km] and “far” [~130km] modes correspond to smaller magnitude and larger magnitude events, respectively. In this figure about $\frac{3}{4}$ of the area under the 10-4 hazard probability density curve corresponds to the “far” event mode, while about $\frac{1}{4}$ of the area corresponds to the “near” mode. Similarly, for the 10-5 hazard the area under the probability density curve is about equal for the “near” and “far” modes. As indicated in SSAR Table 2.5.2-22, the horizontal SSE, as derived following the ASCE 43-05 methodology, is equal to, or only slightly greater than, the 10-4 uniform hazard response spectrum at high frequencies. Therefore, the relative contribution of the “far” and “near” events may be estimated from the 10-4 deaggregation: $\frac{3}{4}$ to $\frac{1}{4}$ or 3:1.

As described above, emphasis in choosing the relative contributions to V/H of “near” and “far” earthquakes was focused on the high-frequency part of the spectrum. The same assessment at the low-

frequency end of the spectrum is not as sensitive to magnitude and distance nor, therefore, to the distinction between “near” and “far” events. And, as discussed in the SSAR and below, the V/H ratio chosen for low-frequency motions was ultimately based on engineering precedent and judgment.

The SRS site-specific soil profile is not published in Lee (2001) so that discussion of similarities and differences between it and the Vogtle ESP soil profile (see SSAR Figure 2.5.4-7) cannot be made. Nevertheless, given the proximity of SRS to the Vogtle ESP site, the site conditions at SRS were assumed likely to be more comparable to those at the Vogtle ESP site than the generic CEUS soil profile used in NUREG/CR-6728. This is the reason the Lee (2001) V/H ratios were considered. Despite expected gross similarities, as well as possible notable smaller-scale differences in soil profiles between SRS and the Vogtle ESP site, the approach used to develop V/H was to use an approximate envelope, rather than an average or weighted average, of the estimates resulting from consideration of Lee (2001) and NUREG/CR-6728 as a guide for the recommended V/H.

As discussed above, relative weights for “near” and “far” event contributions to V/H were considered within each of the two V/H estimates – i.e., NUREG/CR-6728 [SSAR Section 2.5.2.7.1.1] and Lee (2001) [SSAR Section 2.5.2.7.1.2] – however, weights were not applied to the results of the two estimates themselves to derive the final SSE V/H. Rather an approximate envelope of the two results was recommended as an alternative to the generic V/H ratios presented by Reg. Guide 1.60. This is discussed in SSAR Section 2.5.2.7.1.3 and as shown in SSAR Figure 2.5.2-43. From this figure it is clear that the V/H ratios of Lee (2001) have been approximated by two log-log line segments for frequencies between 1 and 100 Hz while for lower frequencies a constant ratio of 0.5 (a value greater than either the Lee or NUREG/CR-6728 in this frequency range) has been recommended. This final log-log line segment smoothing of the approximate envelope of the Lee or NUREG/CR-6728 values is in accord with the type of simple smoothing used in Reg. Guide 1.60, whose frequency-dependent V/H ratio values are also shown in SSAR Figure 2.5.2-43.

Following the response above for the use of the approximate envelope of the two V/H estimates, the recommended V/H in SSAR Figure 2.5.2-43 follows this guidance, except in a range of low frequencies – about 0.25 to 1.0 Hz – where the literal envelop would dip to V/H values less than 0.2.

As discussed above, the intent for the V/H developed for the Vogtle site was to derive more modern and site or region-specific modification of the Reg. Guide 1.60 V/H, maintaining the smooth or simple character of that function. A V/H function with values that drop to less than 0.2 in a narrow range of low frequencies (as do both the Lee (2001) and NUREG/CR-6728 models) would have been a significant departure in shape and amplitude from the Reg. Guide 1.60 V/H which varies very gradually from 0.70 to 0.67 over the same frequency range. Following the literal envelop would have given a vertical SSE that largely eliminated the resonance peak seen in the horizontal SSE at ~0.55 Hz. Given the current lack of a robust methodology for explicitly determining CEUS V/H for soil sites, it was judged to be better to maintain the resonance peak and simple V/H function analogous to that presented in Reg. Guide 1.60.

2.5.3-1 SSAR Sections 2.5.3.1.2 and 2.5.3.1.7 refer to features mapped by McDowell and Houser (1933) and Bartholomew et al. (2002), including “clastic dikes”, that these authors interpreted as possibly related to tectonism during late Eocene to late Miocene. These features are attributed to a non-tectonic origin in SSAR Sections 2.5.3.1.2, 2.5.3.1.7, and 2.5.3.8.2.2 without any discussion of the field evidence for this conclusion.

Please discuss criteria used to determine that these features are non-tectonic in origin and related to pedogenic soil-forming processes, including a comparison with characteristics of clastic dikes mapped in trenches in the site area which are also described as non-tectonic features in the SSAR.

Response:

McDowell and Houser (1983) compiled the locations of small-scale deformation and sedimentary structures in the vicinity of VEGP site and the SRS. They infer that “all of these features ... were produced by gravity-induced deformation as a result of loading, compaction, slump, sliding, or in some cases possibly by tectonic deformation.” Only six localities of “clastic dikes” were listed by McDowell and Houser (1983), who further indicate “the origin of clastic dikes (table 3) is not clear.”

Based on our own reconnaissance of exposures in the Site Area, we have documented abundant “clastic dikes” that have characteristics consistent with a pedogenic or weathering origin, but no features that can reasonably be interpreted to have formed as a result of injected sand. Our field reconnaissance of “clastic dikes” exhibited the following primary characteristics, which were summarized by the Bechtel (1984) study of these features within a large trench exposure on the VEGP site:

1. The dikes are widely distributed through the region in deeply weathered clayey and silty sands of the Eocene Hawthorne and Barnwell Formations.
2. The dikes occur in nearly all exposures of the weathered profile but are rare in exposures of stratigraphically lower, less weathered sediment.
3. The dikes contain a central zone of bleached host rock bounded by a cemented zone of iron oxide. Some dikes contain a clay core.
4. Grain size analyses on samples indicate that the dike interval contains the same grain distribution as the host sediment with slightly more silt and clay (excluding clay core).
5. The dikes and associated mottling decrease downward in density and size. In most cases, the dikes taper downward and pinch-out over a 5- to 15-ft distance.

In contrast to the non-tectonic “clastic dikes”, Bartholomew et al. (2002) describe clastic dikes that cut across poorly bedded clay-rich strata and are filled with massive, medium to coarse sand. They emphasize that these features represent true clastic dikes and not features that have commonly been referred to as “clastic dikes”, a term that has inappropriately been applied for decades to features that are probably related to weathering along joints or fractures. However, the clastic dikes identified by Bartholomew et al. (2002) are syndepositional due to the presence of marine animal burrows that cross cut the dikes.

The formation of these dikes occurred during the late Eocene while the sediments were in a subaqueous marine environment (Bartholomew et al. 2002). Whether these clastic dikes of Bartholomew et al. (2002) formed as a result of seismic shaking or some other process related to soft sediment deformation (e.g., compaction and de-watering), the age of these features is significantly older than Quaternary, and therefore do not reflect geologically recent seismic activity. As previously stated in the SSAR, even if these features are of tectonic origin, they constitute evidence for earthquakes that occurred during or prior to the late Miocene.

The next revision to the ESP application will address as appropriate the information provided in this response.

2.5.3-2 SSAR Sections 2.5.3.8.2.1 and 2.5.3.8.2.2 discuss features interpreted to be non-tectonic in origin that include warped bedding, fractures, small-scale faults, injected sand dikes, and clastic dikes. Warped bedding, fractures, small-scale faults, and injected sand dikes are interpreted to indicate local dissolution of the underlying Utley Limestone and resultant plastic and brittle collapse of overlying Tertiary sediments which occurred more than 10,000 years ago. No formation mechanism is described for the injected sand dikes. The clastic dikes are interpreted to result from weathering and pedogenic soil-forming processes that were enhanced along older fractures initially produced by dissolution of the underlying Utley Limestone.

a. Please describe where these non-tectonic features are located relative to the proposed trace of the Pen Branch Fault at the VEGP site.

b. Please discuss field data, observations, and reasoning which resulted in the conclusion about a dissolution origin for the warped bedding, fractures, small-scale faults, and injected sand dikes, including a specific explanation of the formation mechanism for the injected dikes.

c. Please discuss field data, observations, and reasoning which resulted in the conclusion that the injected sand and clastic dikes do not represent a response to Quaternary or Holocene earthquakes.

Response:

A variety of abundant non-tectonic deformation features were the focus of detailed studies in a large trench at the VEGP site (Bechtel 1984). As shown on SSAR Figure 2.5.1-34, the trench is located within the upper portion of the monocline in the Blue Bluff marl and near the trace of the Pen Branch fault. The trace of the fault shown on SSAR Figure 2.5.1-34 and others in the SSAR is not a surface projection of the fault, but rather the location of the fault where it intersects the contact between basement rock and overlying Coastal Plain deposits. In addition to the features documented in the trench, “clastic dikes” have been observed in other excavations at the site and are likewise concluded to be of non-tectonic origin.

The dissolution origin for the warped bedding, fractures, small-scale faults, “clastic dikes” and sand-injected dikes is interpreted largely from the observations and detailed documentation of these features in a large trench exposure that was over 900 ft long, 30 to 45 ft deep, and 25 to 40 ft across (Bechtel 1984). The high concentration of these features within the trench and the spatial and kinematic relationships between different types of deformation features provide some of the best information regarding their origin (see RAI Figure 2.5.3-2A). Field mapping efforts performed as part of the VEGP ESP application also identified “clastic dikes” within the VEGP site and surrounding site area, and similarly concluded these features are of a non-tectonic origin based on field observations.

As described in Bechtel (1984), “The lateral and vertical dimensions of the trench permitted accurate determination of the relationships of all the structures to one another and to the host sediment, while detailed mapping of both walls provided data for three-dimensional reconstruction and analysis of the structures. In addition, previous VEGP geologic investigations have accurately defined the subsurface stratigraphy at the site.” For this RAI response, much of the description of the features and field relationships observed in the trench exposure are taken from the Bechtel (1984) report.

Evidence for dissolution (extensive leaching and solution cavities) of the Utley limestone at the site is well-documented (USNRC 1985). The Utley limestone lies below the Eocene sands, in which the small deformational features occur, and directly above the Blue Bluff marl. Due to the evidence of dissolution,

the Utley limestone and overlying deposits were excavated and removed for Units 1 and 2 and will also be removed for the construction of Units 3 and 4.

The 3-dimensional nature of the warped bedding, combined with the spatial and kinematic relationships of the small-scale faults and fractures along the margins of the more strongly warped depressions, clearly demonstrates a dissolution or sediment collapse origin. The highly irregular, discontinuous nature of folding is consistent with a non-tectonic dissolution origin and inconsistent with a tectonic origin, since there are no laterally persistent fold axes (see RAI Figure 2.5.3-2B following this response). If this minor fold deformation was associated with the underlying Pen Branch fault, fold axes should be laterally persistent and parallel to the fault. The discontinuous nature of domes and depressions in an “egg carton” or “dimpled” pattern reflects the more random, non-tectonic process of dissolution. The concentration of fractures and small normal faults at the margins of the structural lows (Sta 450 in RAI Figure 2.5.3-2A following this response) illustrates that the minor folding is a result of dissolution collapse in underlying strata, as opposed to localized, differential uplift of the domes.

Most of the small-scale faults have normal displacement toward or into the depressions and a few exhibit minor reverse slip near the crests of some arches (Bechtel 1984). These features are of limited dimensions and cannot be traced laterally across the width of the trench. The orientations of fractures and small faults are locally consistent with the limbs of the individual arches and depressions, but vary strongly from fold to fold. In some cases, such as Sta 450 in RAI Figure 2.5.3-2B, the small faults actually arc over the centers of some of the depressions. These field relationships all support an origin related to very localized settlement of the depressions resulting from dissolution and collapse of underlying strata.

A true clastic dike is formed by injection of sand into a fracture from a source stratigraphically above or below. The term “clastic dike” has been widely mis-used in the literature to describe features that, based on observations from the Bechtel (1984) trench and other studies, including the ESP project, formed primarily as a result of weathering and soil-forming processes. Some of the principal reasons that “clastic dikes” do not represent features produced from earthquake ground shaking are summarized by Bechtel (1984) as:

1. The dikes are widely distributed through the region in deeply weathered clayey and silty sands of the Eocene Hawthorne and Barnwell Formations.
2. The dikes occur in nearly all exposures of the weathered profile but are rare in exposures of stratigraphically lower, less weathered sediment.
3. The dikes contain a central zone of bleached host rock bounded by a cemented zone of iron oxide. Some dikes contain a clay core.
4. Grain size analyses on samples indicate that the dike interval contains the same grain distribution as the host sediment with slightly more silt and clay (excluding clay core).

The dikes and associated mottling decrease downward in density and size. In most cases, the dikes taper downward and pinch-out over a 5- to 15-foot distance. RAI Figure 2.5.3-2C following this response shows an example of downward termination of a “clastic dike” in a large quarry exposure near the meteorological tower in the southern portion of the VEGP site. RAI Figure 2.5.3-2C also shows the decrease in small dikes and mottling downward from the more strongly developed soil at the ground surface.

The injected sand dikes occur at three localities in the trench and were not observed at any other location either on or off the VEGP site during the ESP mapping effort. The sand dikes, as identified by Bechtel

AR-07-0801
Enclosure 1
RAI Response

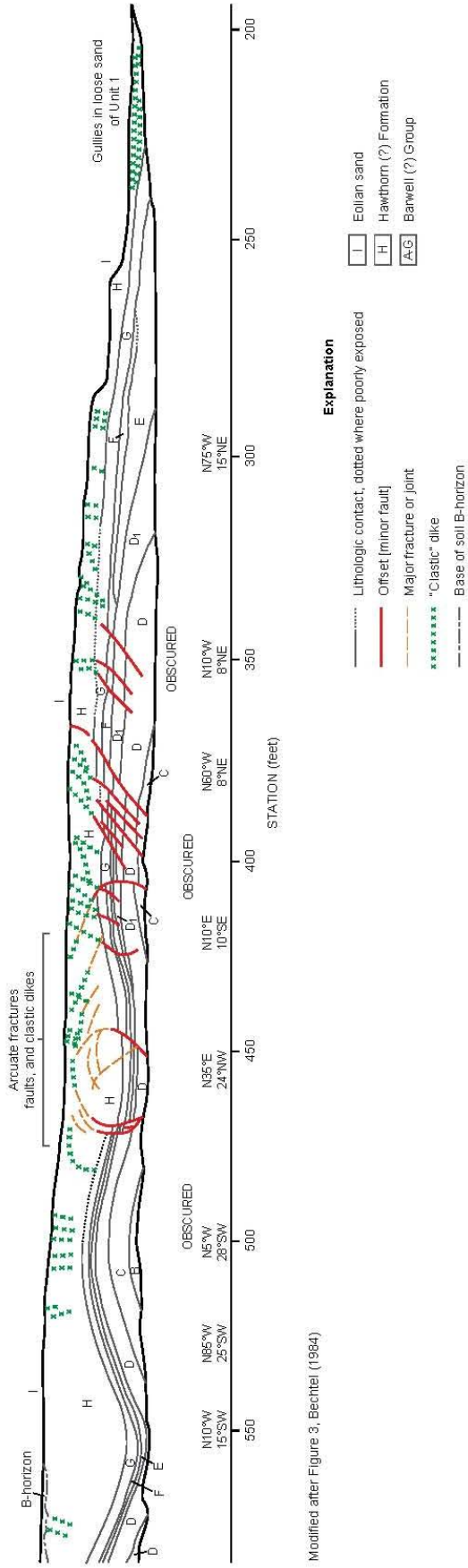
(1984), consist of lavender, loosely consolidated, well sorted, very fine, clean quartz sand and are confined to a single unit (Unit D) within the trench. These dikes were likely formed by fluid or plastic injection of a source sand from underlying sand beds of Unit C. The close spatial association of the sand dikes with limbs of the depressions suggests that the liquid injection resulted from development of the depression.

The injected sand dikes and “clastic dikes” are estimated to be of significant age. The sand dikes are interpreted to have formed from an early phase of sediment collapse following the Eocene deposition of the strata and prior to the development fracturing, jointing, and minor faulting associated with a subsequent sediment collapse that resulted in the formation of small faults that offset the sand dikes. The sand dikes predate a Miocene erosional event. The “clastic dikes” are interpreted to be younger than the sand dikes. “Clastic dikes” probably developed during a major weathering event that produced the relict paleosol on Unit H and are thus older than (1) middle to late Pleistocene erosion event of Unit H paleosol and (2) deposition of the late Pleistocene and Holocene eolian sand of Unit I (Bechtel 1984). The SER (USNRC 1985) concluded that the “clastic dikes” are likely great in age and that “there is no evidence that these features represent a safety issue for the plant, whatever their origin.”

References

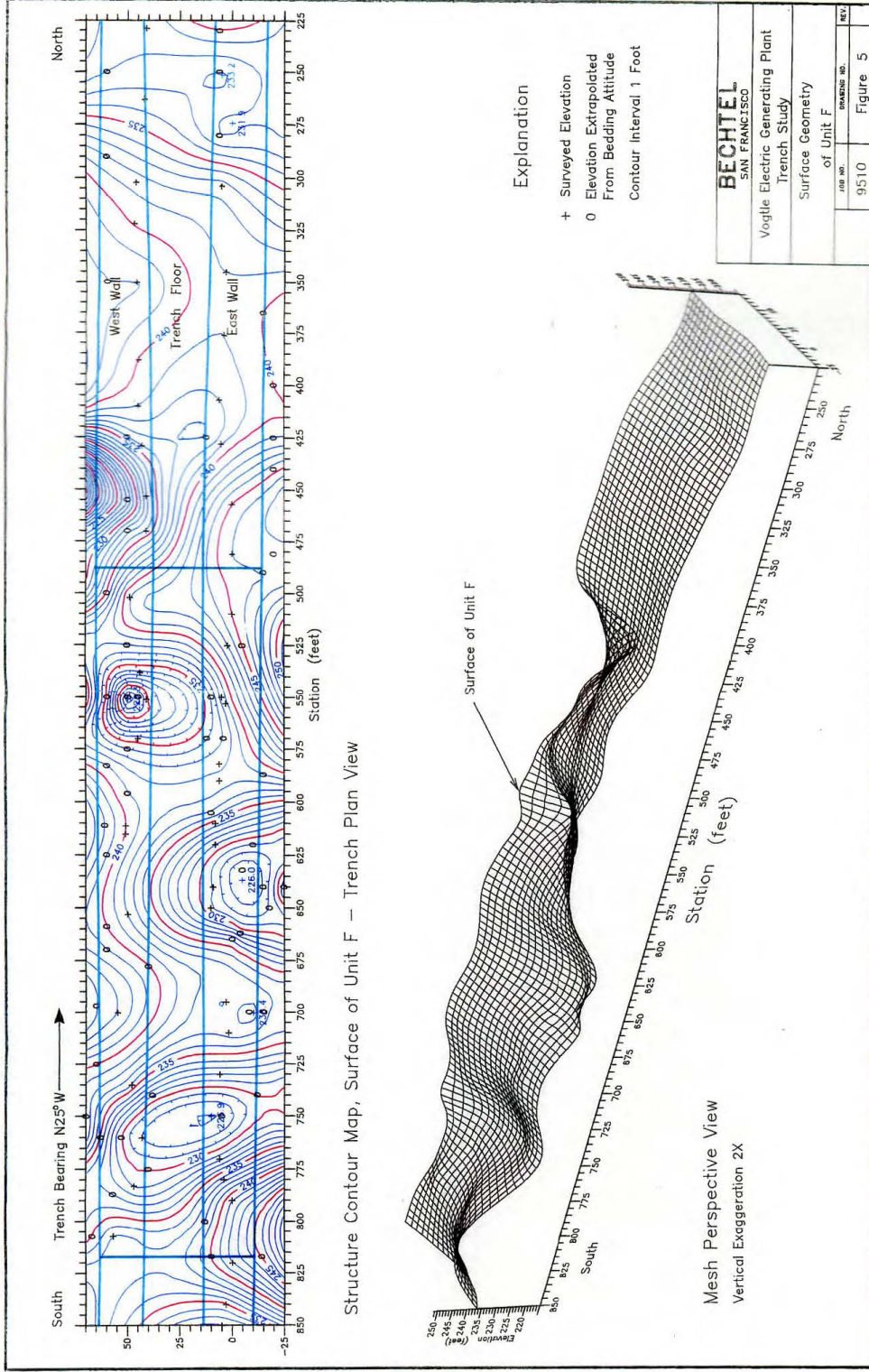
(USNRC 1985) US Nuclear Regulatory Commission, Safety Evaluation Report related to the operation of Vogtle Electric Generating Plant, Units 1 and 2, Docket Nos. 50-424 and 50-425, June 1985.

The next revision to the ESP application will address as appropriate the information provided in this response.



Modified after Figure 3, Bechtel (1984)

RAI Figure 2.5.3-2A Photo Mosaic and Geologic Interpretation of a Portion Trench, West Wall



RAI Figure 2.5.3-2B. Surface Geometry of Unit F Illustrating Localized Nature of Deformation